

CME 300 Properties of Materials

Monday, Wednesday, Friday 9:00 to 9:50
Swift 619

Dr. Greg Beaucage

492 Rhodes Hall (410 Rhodes Hall Lab)

beaucag@uc.edu

556-3063

Office Hours: Monday and Wednesday 10:00 to 11:00 or by
arrangement

Suggested Texts:

- 1) *Materials Science and Engineering an Introduction*, W. D. Callister (and D. G. Rethwisch) any edition
- 2) *Understanding Materials Science*, R. E. Hummel

Engineer in Training (EIT) or Fundamentals of Engineering (FE) Exam

Mathematics

Engineering Probability and Statistics

Chemistry

Computers

Ethics and Business Practices

Engineering Economics

Engineering Mechanics (Statics and Dynamics)

Strength of Materials

Material Properties

Fluid Mechanics

Electricity and Magnetism

Thermodynamics

Chemical Engineers will run into materials if they work in:

plastics (70% of Chemists and Chemical Engineers)

metals (5%)

consumer products

microelectronics

heterogeneous catalysts

AIChE Annual Meeting

Browse by Group/Topical

01 Engineering Sciences and Fundamentals

02 Separations Division

03 Particle Technology Forum

04 Education

05 Management Division

06 North American Mixing Forum

07 Energy and Transport Processes

08 Materials Engineering and Sciences Division

09 Environmental Division

10 Computing and Systems Technology Division

11 Safety and Health Division

12 Process Development Division

14 Nuclear Engineering Division

15 Food, Pharmaceutical & Bioengineering Division

16 Fuels and Petrochemicals Division

17 Forest and Plant Bioproducts Division

18 Liaison Functions

20 Catalysis and Reaction Engineering Division

21 Computational Molecular Science and Engineering Forum

22 Nanoscale Science and Engineering Forum

23 Sustainable Engineering Forum

24 Chemical Engineering & the Law Forum

T1 Topical 1: Water Technology for Developed and Developing Countries (see also Separations Division)

T3 Topical 3: 2011 Annual Meeting of the American Electrophoresis Society (AES)

T4 International Congress on Energy 2011

T5 Topical 5: Nanomaterials for Energy Applications

T9 Topical 9: Sensors

TA Topical A: Systems Biology

TB 1st Annual World Congress on Sustainable Engineering

TC Topical C: Environmental Aspects, Applications, and Implications of Nanomaterials and Nanotechnology

TI Topical I: Comprehensive Quality by Design in Pharmaceutical Development and Manufacture



Course Logistics and Grading

Every three classes a quiz ~ 30 minutes
9-10 quizzes per quarter

Mandatory comprehensive final exam worth four quizzes

Drop three quiz grades

If you do not drop a quiz grade, you can skip the final

Homework will be assigned but not collected

Only whole grades and no grade scaling

A = 90 or above

B = 80 or above

C = 70 or above

D = 60 or above

F = below 60

Academic Honesty:

If you cheat you receive an F for the course

Appeals are to the college academic standards committee

We consider three types of materials

Metals

Ceramics, Semiconductors

Polymers, Gels, Rubbers, Plastics

Biomaterials, Nanomaterials, ...

The three types of materials parallel the three fundamental bonds:

Metallic, Ionic, Covalent

(Except for polymers.)

How did this develop historically?

Hummel Chapter I: The first materials

Naturally occurring copper metal (Michigan)

But for the most part metals occur in nature as an oxide in rocks

Clay was used by early man ~ 12,000 years ago

Firing of clay in open fires occurred by accident

Later it was found that hotter flames lead to water resistant ceramics

Metal oxide and sulfide pigments were used in ceramics

In a high temperature (above the melting point) reducing (no oxygen) flame

We can smelt the oxide ore to produce a ground state metal

Addition of fluxing agent (iron ore) can enhance the metal produced

So metallurgy was developed naturally from ceramics in a variety of locations by 5,000 BC

At the earliest stages of human civilization man had ceramics, metals and natural polymers/fibers

What is a metal?

Group →	1	2	3	4	5	6	7	8	9	10	11	12	13	14	15	16	17	18							
↓ Period																									
1	1 H																	2 He							
2	3 Li	4 Be											5 B	6 C	7 N	8 O	9 F	10 Ne							
3	11 Na	12 Mg											13 Al	14 Si	15 P	16 S	17 Cl	18 Ar							
4	19 K	20 Ca	21 Sc	22 Ti	23 V	24 Cr	25 Mn	26 Fe	27 Co	28 Ni	29 Cu	30 Zn	31 Ga	32 Ge	33 As	34 Se	35 Br	36 Kr							
5	37 Rb	38 Sr	39 Y	40 Zr	41 Nb	42 Mo	43 Tc	44 Ru	45 Rh	46 Pd	47 Ag	48 Cd	49 In	50 Sn	51 Sb	52 Te	53 I	54 Xe							
6	55 Cs	56 Ba		72 Hf	73 Ta	74 W	75 Re	76 Os	77 Ir	78 Pt	79 Au	80 Hg	81 Tl	82 Pb	83 Bi	84 Po	85 At	86 Rn							
7	87 Fr	88 Ra		104 Rf	105 Db	106 Sg	107 Bh	108 Hs	109 Mt	110 Ds	111 Rg	112 Uub	113 Uut	114 Uuq	115 Uup	116 Uuh	117 Uus	118 Uuo							
				Lanthanides							57 La	58 Ce	59 Pr	60 Nd	61 Pm	62 Sm	63 Eu	64 Gd	65 Tb	66 Dy	67 Ho	68 Er	69 Tm	70 Yb	71 Lu
				Actinides							89 Ac	90 Th	91 Pa	92 U	93 Np	94 Pu	95 Am	96 Cm	97 Bk	98 Cf	99 Es	100 Fm	101 Md	102 No	103 Lr

Metals

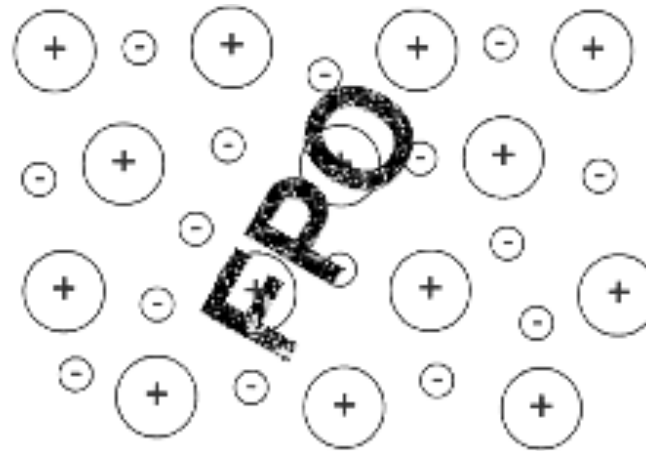
Readily lose electrons and form cations, and ionic bonds with non-metals NaCl
 In the ground state metals lose electrons to form positive ions in a “sea of delocalized electrons”

Ground state metals are produced from oxide ore by reduction when a reducing agent exists
 (iron, copper)
 or by electrolysis (aluminum, sodium)

Mobility of positive ions

from Hummel Text p. 30

FIGURE 3.5. Schematic representation of metallic bonding. The valence electrons become disassociated with "their" atomic core and form an electron "sea" that acts as the binding medium between the positively charged ions.



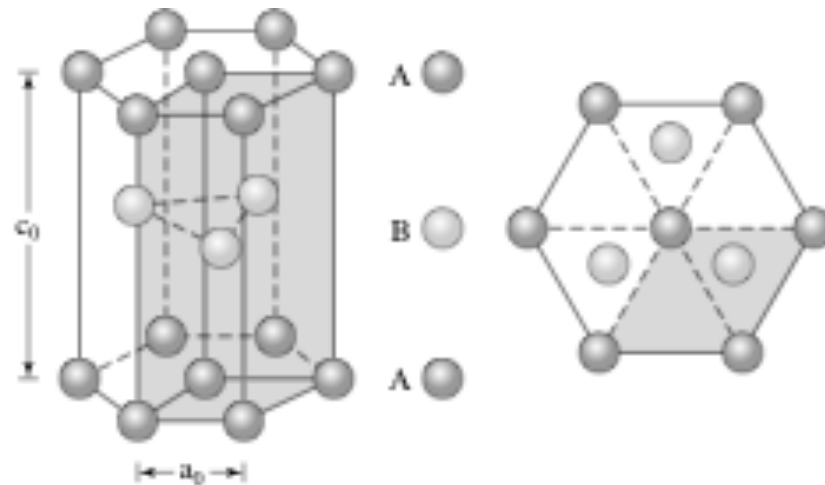
Disordered Liquid State

Ordered Crystalline State

Hexagonal Close Packed Metals (HCP)

from Hummel Text p. 34

FIGURE 3.9. Hexagonal close-packed (HCP) crystal structure. The sixfold symmetry of the lattice is evident. One unit cell is shaded for clarity. There are three crystallographically equivalent possibilities for this unit cell. The stacking sequence (ABA), which will be explained later, is also depicted.



Zn, Mg, Be, α -Ti, Cd, Zr

Brittle Metals

Cannonball Packing

Comparison between hcp and fcc

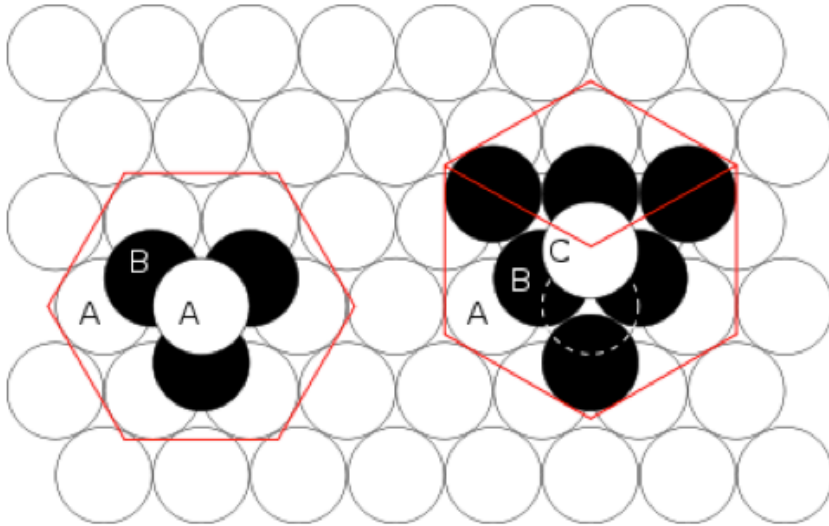


Figure 1 – The hcp lattice (left) and the fcc lattice (right). The outline of each respective Bravais lattice is shown in red. The letters indicate which layers are the same. There are two "A" layers in the hcp matrix, where all the spheres are in the same position. All three layers in the fcc stack are different. Note the fcc stacking may be converted to the hcp stacking by translation of the upper-most sphere, as shown by the dashed outline.

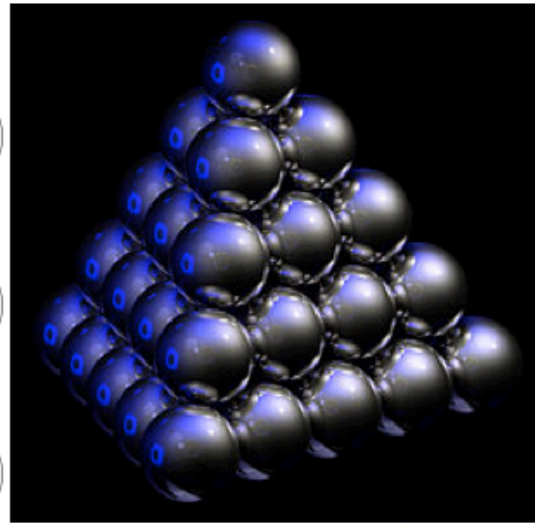


Figure 2 – Thomas Harriot, circa 1585, first pondered the mathematics of the cannonball arrangement or cannonball stack, which has an fcc lattice. Note how adjacent balls along each edge of the regular tetrahedron enclosing the stack are all in direct contact with one another. This does not occur in an hcp lattice, as shown in Fig. 3.

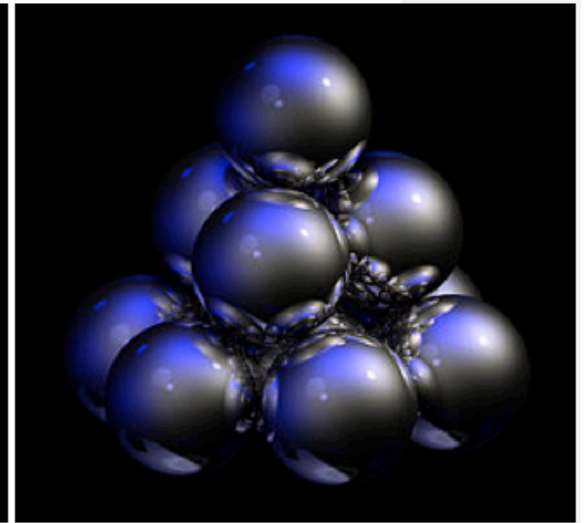


Figure 3 – Shown here is a stack of eleven spheres of the hcp lattice illustrated in Fig. 1. The hcp stack differs from the top 3 tiers of the fcc stack shown in Fig. 2 only in the lowest tier; it can be modified to fcc by an appropriate rotation or translation.

http://en.wikipedia.org/wiki/Close-packing_of_spheres

Formation and Motion of Crystalline Defects are the Source of Mechanical Properties in Many Metals

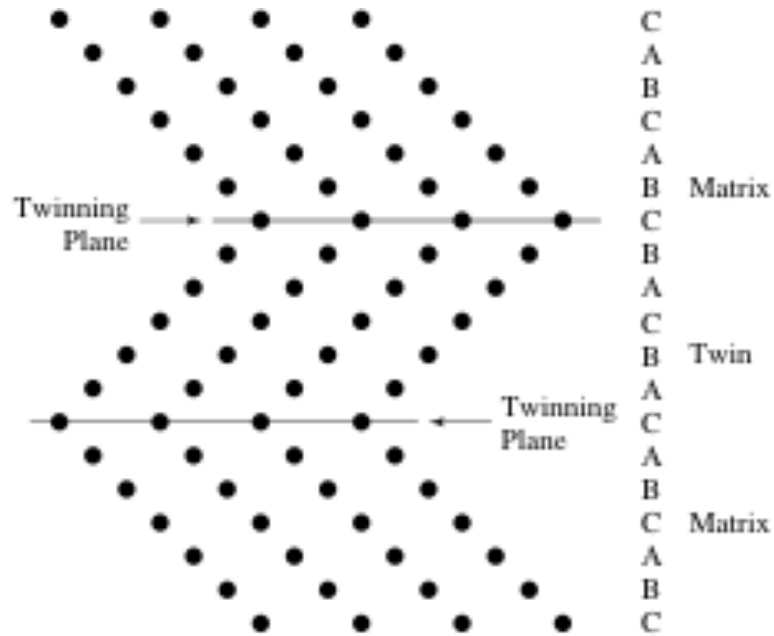


FIGURE 3.12. Stacking faults in an FCC metal to yield twinning. The matrix and the twin match at the interface, called the twinning plane. The figure shows a $(1\bar{1}0)$ plane normal to the (111) twin plane, as we shall explain below.

Hummel

Annealing Twins
Deformation Twins
One reason FCC metals are ductile.

Crystallographic Structures (14 Bravais Lattices)

Hummel P. 33

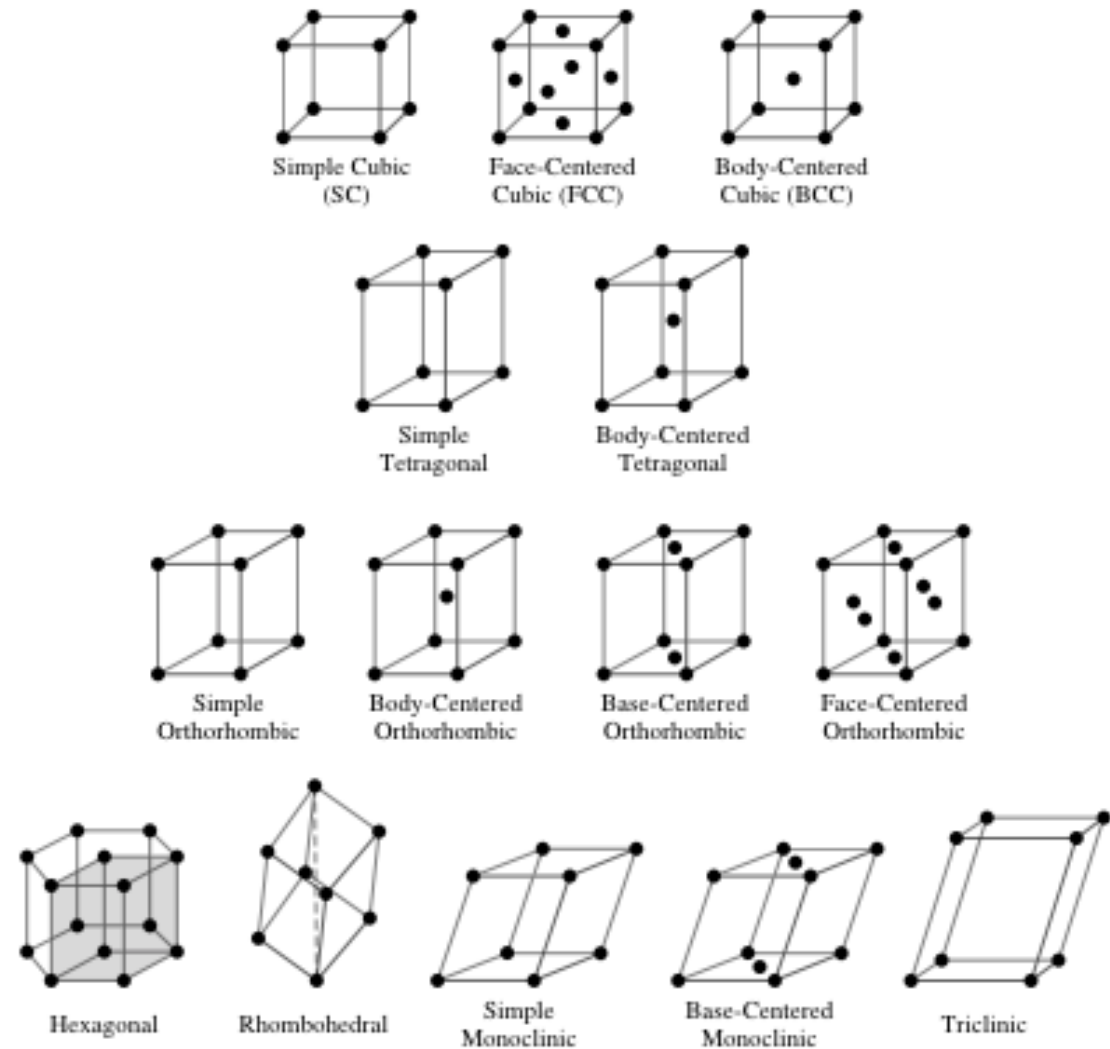
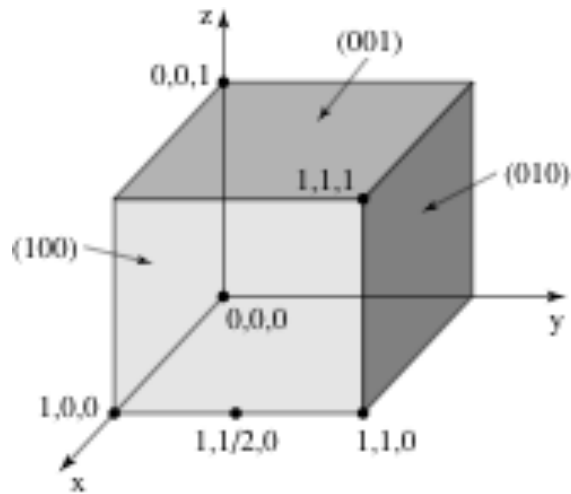


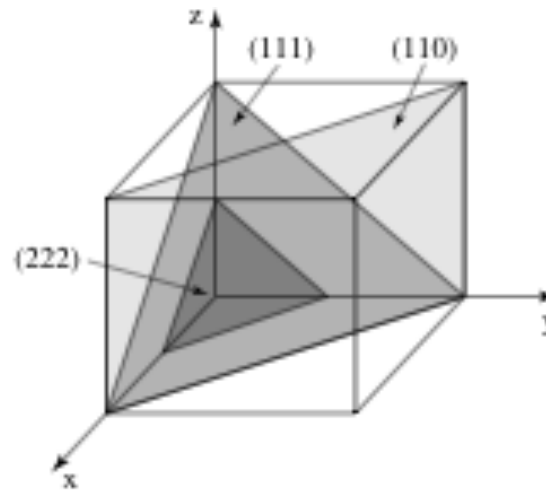
FIGURE 3.8. The 14 Bravais lattices grouped into seven crystal systems:

First row: $a = b = c$, $\alpha = \beta = \gamma = 90^\circ$ (cubic);
 Second row: $a = b \neq c$, $\alpha = \beta = \gamma = 90^\circ$ (tetragonal);
 Third row: $a \neq b \neq c$, $\alpha = \beta = \gamma = 90^\circ$ (orthorhombic);
 Fourth row: at least one angle is $\neq 90^\circ$. *Specifically:*
 Hexagonal: $\alpha = \beta = 90^\circ$, $\gamma = 120^\circ$, $a = b \neq c$ (the unit cell is the shaded part of the structure);
 Rhombohedral: $a = b = c$, $\alpha = \beta = \gamma \neq 90^\circ \neq 60^\circ \neq 109.5^\circ$;
 Monoclinic: $\alpha = \gamma = 90^\circ$, $\beta \neq 90^\circ$, $a \neq b \neq c$;
 Triclinic: $\alpha \neq \beta \neq \gamma \neq 90^\circ$, $a \neq b \neq c$.

In the FCC lattice where is the “closest-packed” hexagonal plane?



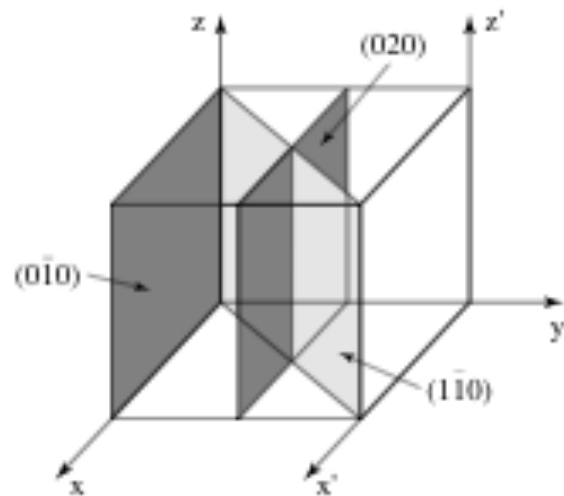
(a)



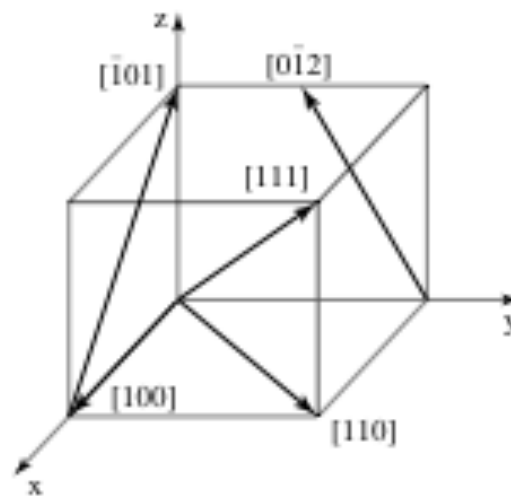
(b)

Miller Indices are 1/intercept
(CURVED BRACKETS)
{FAMILY OF PLANES}

So you don't get infinity



(c)



(d)

Directions are the intercepts
[SQUARE BRACKETS]
<FAMILY OF DIRECTIONS>

In the FCC lattice where is the “closest-packed” hexagonal plane?

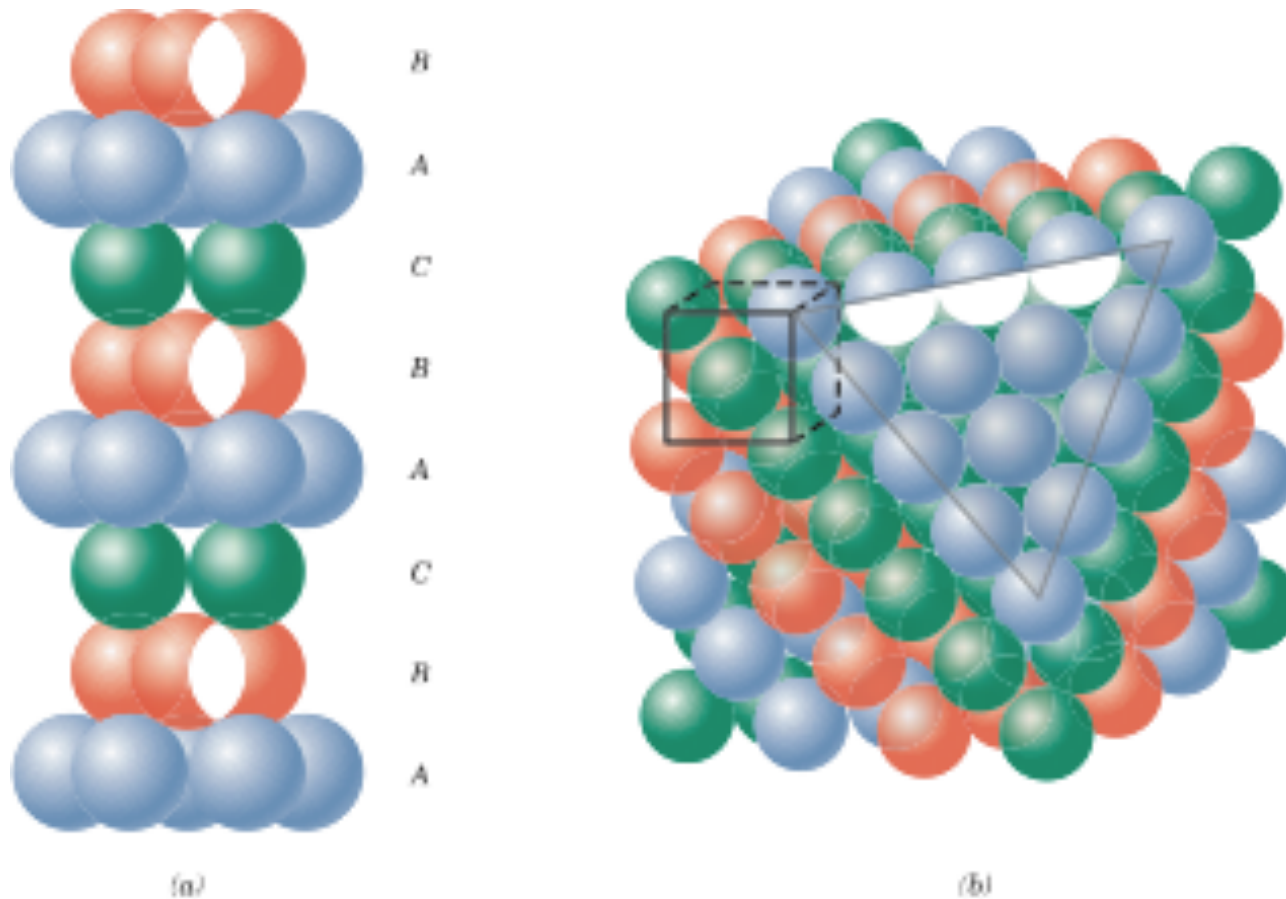


Figure 3.15 (a) Close-packed stacking sequence for face-centered cubic. (b) A corner has been removed to show the relation between the stacking of close-packed planes of atoms and the FCC crystal structure; the heavy triangle outlines a (111) plane. [Figure (b) from W. G. Moffatt, G. W. Pearsall, and J. Wulff, *The Structure and Properties of Materials*, Vol. I, *Structure*, p. 51. Copyright © 1964 by John Wiley & Sons, New York. Reprinted by permission of John Wiley & Sons, Inc.]

Callister P. 63

(111) Plane
or
{111} Family of Planes

For the Hexagonal CP
(0001)

Table 3.1 Atomic Radii and Crystal Structures for 16 Metals

<i>Metal</i>	<i>Crystal Structure^a</i>	<i>Atomic Radius^b</i> (nm)	<i>Metal</i>	<i>Crystal Structure</i>	<i>Atomic Radius</i> (nm)
Aluminum	FCC	0.1431	Molybdenum	BCC	0.1363
Cadmium	HCP	0.1490	Nickel	FCC	0.1246
Chromium	BCC	0.1249	Platinum	FCC	0.1387
Cobalt	HCP	0.1253	Silver	FCC	0.1445
Copper	FCC	0.1278	Tantalum	BCC	0.1430
Gold	FCC	0.1442	Titanium (α)	HCP	0.1445
Iron (α)	BCC	0.1241	Tungsten	BCC	0.1371
Lead	FCC	0.1750	Zinc	HCP	0.1332

^a FCC = face-centered cubic; HCP = hexagonal close-packed; BCC = body-centered cubic.

^b A nanometer (nm) equals 10^{-9} m; to convert from nanometers to angstrom units (\AA), multiply the nanometer value by 10.

For the most part we have HCP, FCC, and BCC crystals in metals

Coordination Number

The **coordination number** is the number of nearest neighbors to a given atom. For example, the center atom in a BCC structure [Figures 3.8 and 3.10(a)] has eight nearest atoms. Its coordination number is therefore 8. The coordination numbers for some crystal structures are listed in Table 3.2.

Atoms per Unit Cell

The **number of atoms per unit cell** is counted by taking into consideration that corner atoms in cubic crystals are shared by eight unit cells and face atoms are shared by two unit cells. They count therefore only 1/8 and 1/2, respectively. As an example, the number of atoms associated with a BCC structure (assuming only one atom per lattice point) is $8 \times 1/8 = 1$ corner atom and one (not shared) center atom, yielding a total of two atoms per unit cell. In contrast to this, an FCC unit cell has four atoms ($8 \times 1/8 + 6 \times 1/2$). The FCC unit cell is therefore more densely packed with atoms than the BCC unit cell; see also Table 3.2.

Packing Factor

The **packing factor**, P , is that portion of space within a unit cell which is filled with spherical atoms that touch each other, i.e.:

$$P = \frac{A_{uc} \cdot V_A}{V_{uc}}, \quad (3.1)$$

TABLE 3.2. Some parameters and properties of different crystal structures

Crystal structure	Coordination number	Atoms per unit cell	Packing factor	Mechanical properties
HCP	12*	2	0.74*	Brittle
FCC	12	4	0.74	Ductile
BCC	8	2	0.68	Hard
Simple cubic (SC)	6	1	0.52	No representative materials

*Assuming a c/a ratio of 1.633.

Hummel P. 34

For Cubic Crystals (FCC, BCC)

Interplanar Spacing

The distance between parallel and closest neighboring lattice planes which have identical Miller indices is given for cubic materials by:

$$d_{hkl} = \frac{a_0}{\sqrt{h^2 + k^2 + l^2}}, \quad (3.3)$$

where a_0 is the lattice constant (see above) and hkl are the Miller indices of the planes in question. More complex expressions exist for other crystal systems.

atom positions. The aggregate of atoms in Figure 3.1c represents a section of crystal consisting of many FCC unit cells. These spheres or ion cores touch one another across a face diagonal; the cube edge length a and the atomic radius R are related through

$$a = 2R\sqrt{2} \quad (3.1)$$

of BCC unit cells with the atoms represented by hard sphere and reduced-sphere models, respectively. Center and corner atoms touch one another along cube diagonals, and unit cell length a and atomic radius R are related through

$$a = \frac{4R}{\sqrt{3}} \quad (3.3)$$

From Hummel

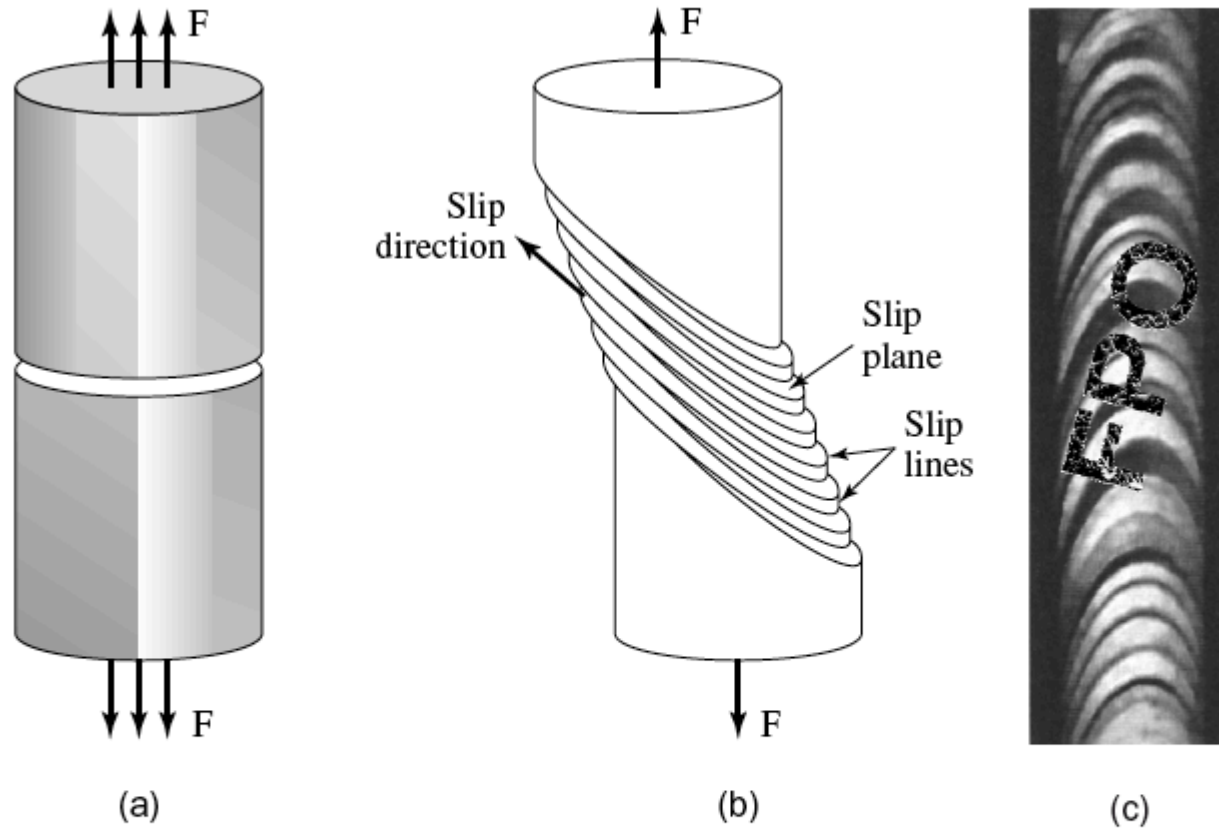
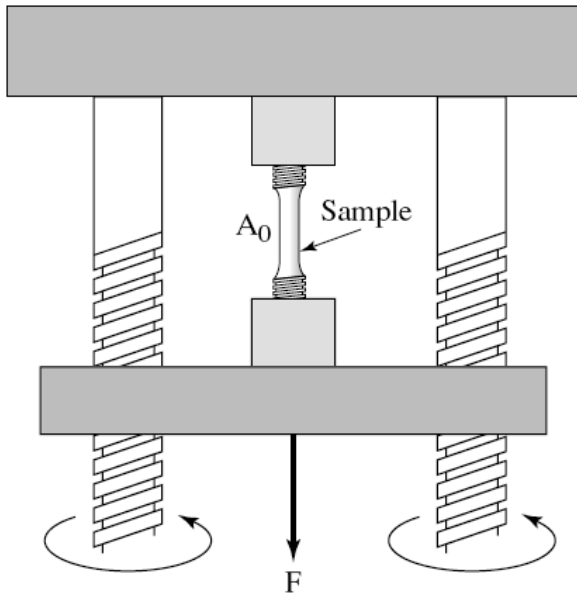


FIGURE 3.19. Schematic representation of two mechanisms by which a single crystal is assumed to be stretched when applying a force, F : (a) breaking interatomic bonds, (b) considering slip, and (c) photomicrograph of slip bands in a single crystal of zinc stressed at 300°C . Adapted from *Z. Phys.* **61**, 767 (1930).

Slip Planes
Critically Resolved Shear Stress



Hummel P. 13

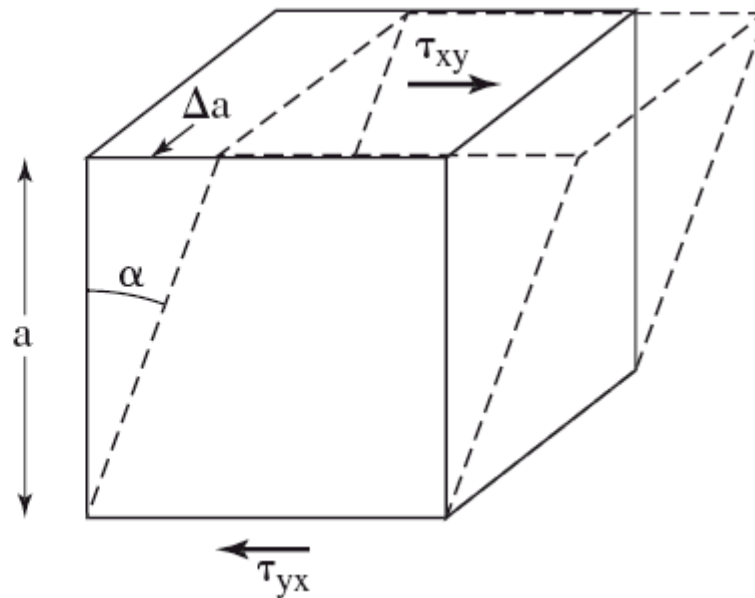
FIGURE 2.2. Schematic representation of a tensile test equipment. The lower cross-bar is made to move downward and thus extends a force, F , on the test piece whose cross-sectional area is A_0 . The specimen to be tested is either threaded into the specimen holders or held by a vice grip.

$$\text{Stress} = \sigma_{ij} = dF_i/dA_j$$

For Shear the symbol is often τ_{ij}

$$\text{Strain} = \epsilon_{ij} = dl_i/dl_j$$

FIGURE 2.3. Distortion of a cube caused by shear stresses τ_{xy} and τ_{yx} .



Hummel P. 14

Stress/Strain: Vectors and Tensors

A vector has magnitude and direction

Force is a vector: $\bar{F}_x, \bar{F}_y, \bar{F}_z$

Area can be described as a vector with magnitude of the area and direction of the normal: $\bar{A}_x, \bar{A}_y, \bar{A}_z$

Length is a vector: $\bar{u}_x, \bar{u}_y, \bar{u}_z$

Direction is a vector: $\bar{x}_x, \bar{x}_y, \bar{x}_z$

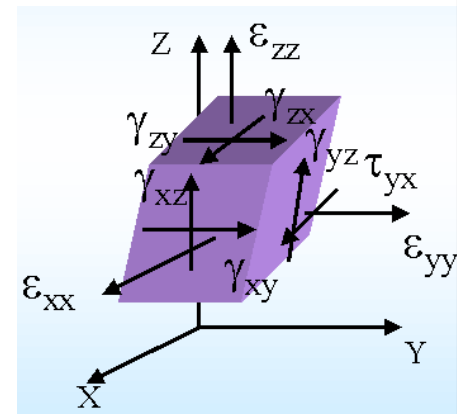
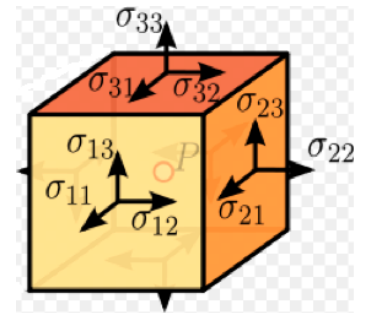
A tensor relates two (or more) vectors (and scalars)

Stress is a two-dimensional tensor (9 components): $\bar{\tau}_{ij} = \bar{\sigma}_{ij} = \frac{\partial \bar{F}_i}{\partial \bar{A}_j}$

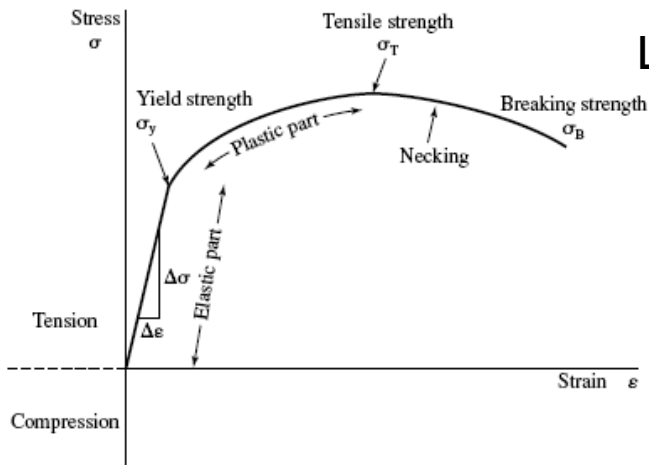
Strain is a two-dimensional tensor (9 components): $\bar{\gamma}_{ij} = \bar{\epsilon}_{ij} = \frac{\partial \bar{u}_i}{\partial \bar{x}_j}$

*Due to symmetry only 6 components are independent
(There are other simplifying rules)*

$$\epsilon_{ij} = \begin{bmatrix} \epsilon_{xx} & \gamma_{xy} & \gamma_{xz} \\ \gamma_{yx} & \epsilon_{yy} & \gamma_{yz} \\ \gamma_{zx} & \gamma_{zy} & \epsilon_{zz} \end{bmatrix}$$



Stress/Strain Plots (Solids)



Hooke's Law:
Linear Response

Tensile $\bar{\sigma}_{11} = E\bar{\epsilon}_{11}$

E = Tensile (Young's)
Modulus

Shear $\bar{\tau}_{12} = G\bar{\gamma}_{12}$

G = Shear Modulus

At high strains non-linear behavior is seen
This (usually) indicates permanent deformation or yielding
This occurs at the yield point (yield stress/yield strain)

Stress/Rate of Strain Plots (Fluids)

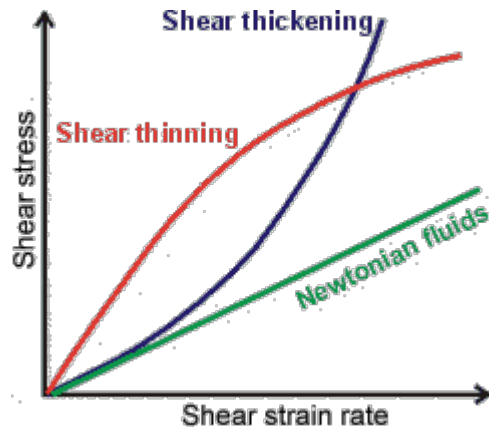
Strain rate is the same as the velocity gradient

$$\dot{\gamma}_{ij} = \frac{\partial \dot{\gamma}_{ij}}{\partial t} = \frac{\partial \left(\frac{\partial \bar{u}_i}{\partial \bar{x}_j} \right)}{\partial t} = \frac{\partial \left(\frac{\partial \bar{u}_i}{\partial t} \right)}{\partial \bar{x}_j} = \frac{\partial \bar{v}_i}{\partial \bar{x}_j}$$

Fluids can not hold a stress
they instantly (or quickly) "relax"

Hence: $E = G = 0$

Fluids resist stress through viscosity, η
This is measured in a dynamic measurement



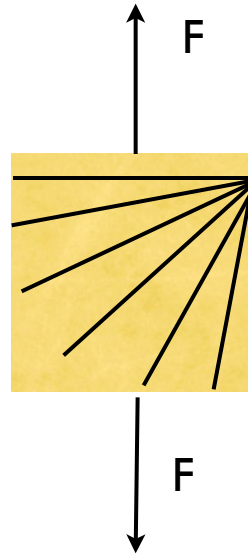
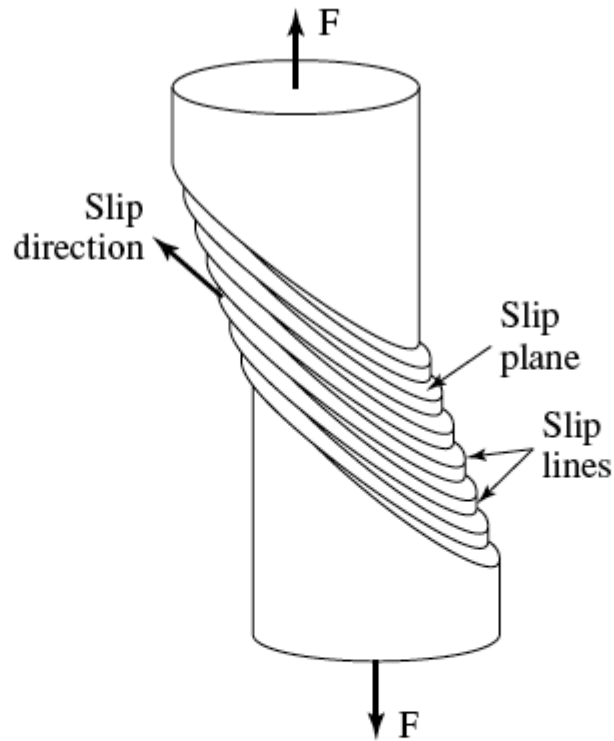
Newton's Law:
Linear Response

Viscosity is usually
measured in shear:

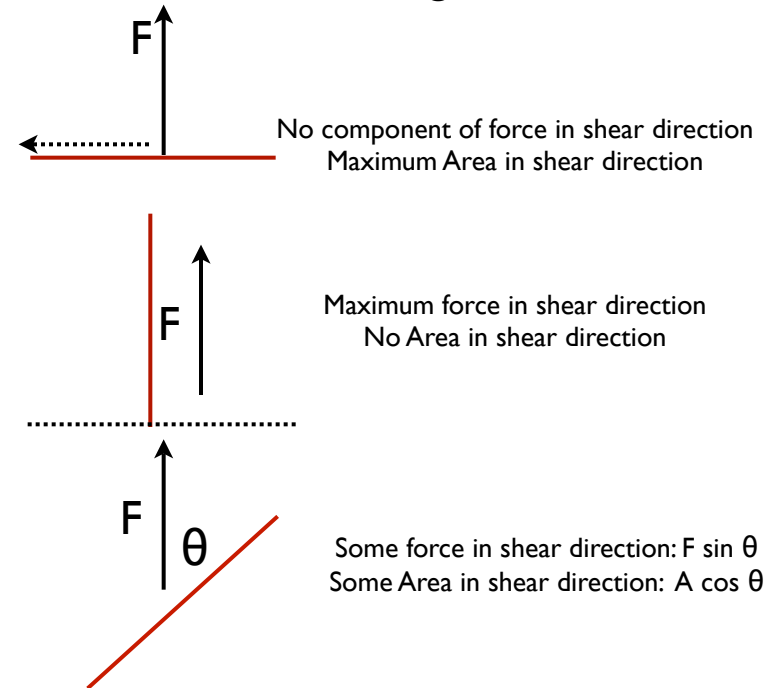
$$\bar{\tau}_{12} = \eta \dot{\gamma}_{12}$$

At high strain rates non-linear behavior is seen
This indicates changes in the fluid structure under strain

Why 45°?



Planes on which shear might occur



Like a sail in the wind.

Schmidt's Law

Hummel P. 60

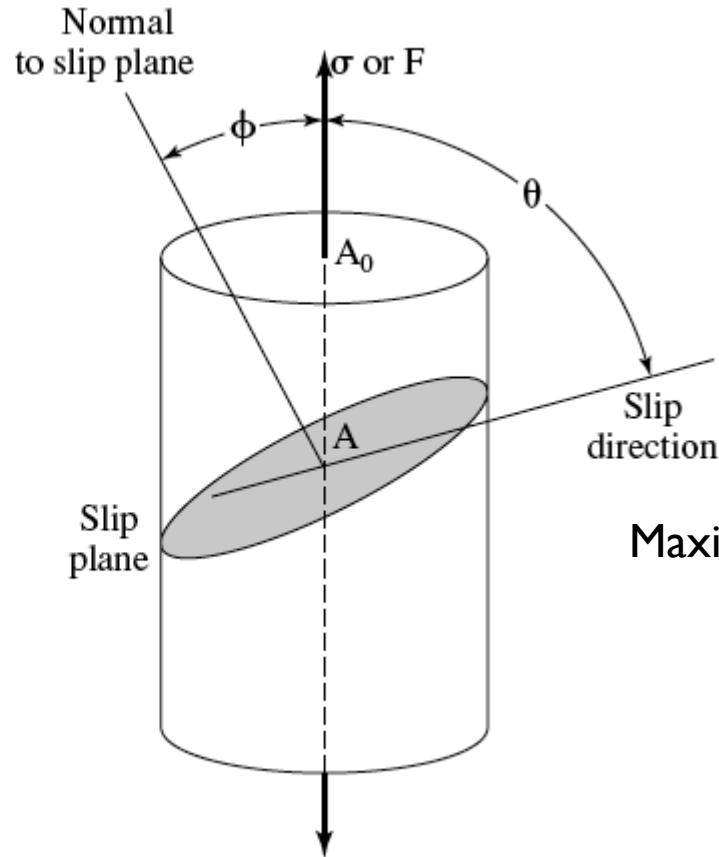


FIGURE 3.27. A slip plane normal is shown under an angle ϕ to an applied force (or stress). Note: $\phi + \theta$ is usually *not* equal to 90° . The two angles are not necessarily in the same plane.

$$\tau_y = \sigma \cos \phi \cos \theta.$$

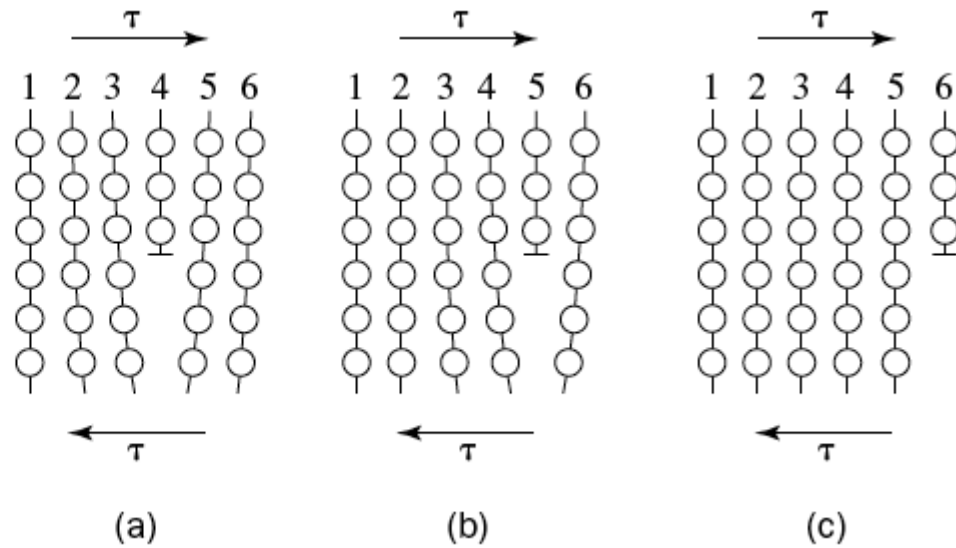
Maximum occurs at 45° for both angles $\sigma/2$

$$\sigma_0 = \frac{\tau_0}{\cos \phi \cos \theta},$$

$$\sigma_0 = 3\tau_0.$$

Hummel P. 48

FIGURE 3.20. Simplified two-dimensional representation of an edge dislocation and of dislocation movement under the influence of a shear stress, τ , in a single crystalline, cubic-primitive lattice. A $\{100\}$ plane is depicted. The shear stress is shown to be applied parallel to the slip plane and normal to the dislocation line (see Figure 3.21).



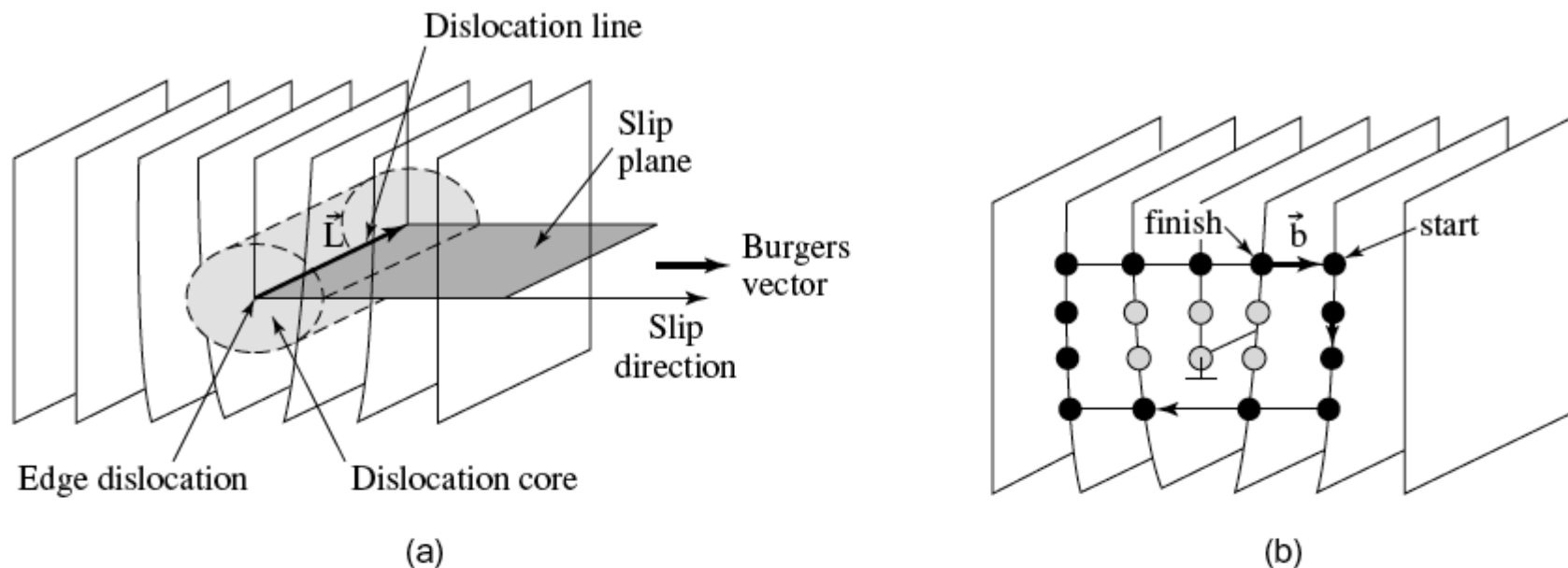


FIGURE 3.21. (a) Definition of slip direction, slip plane, Burgers vector, dislocation line, and dislocation core for an edge dislocation in a cubic primitive lattice [compare to Figure 3.19(b)]. Note that the edge dislocation slips in its slip plane, which is situated *between* two neighboring atomic planes. (b) Construction of a “right-hand finish to start” Burgers vector.”

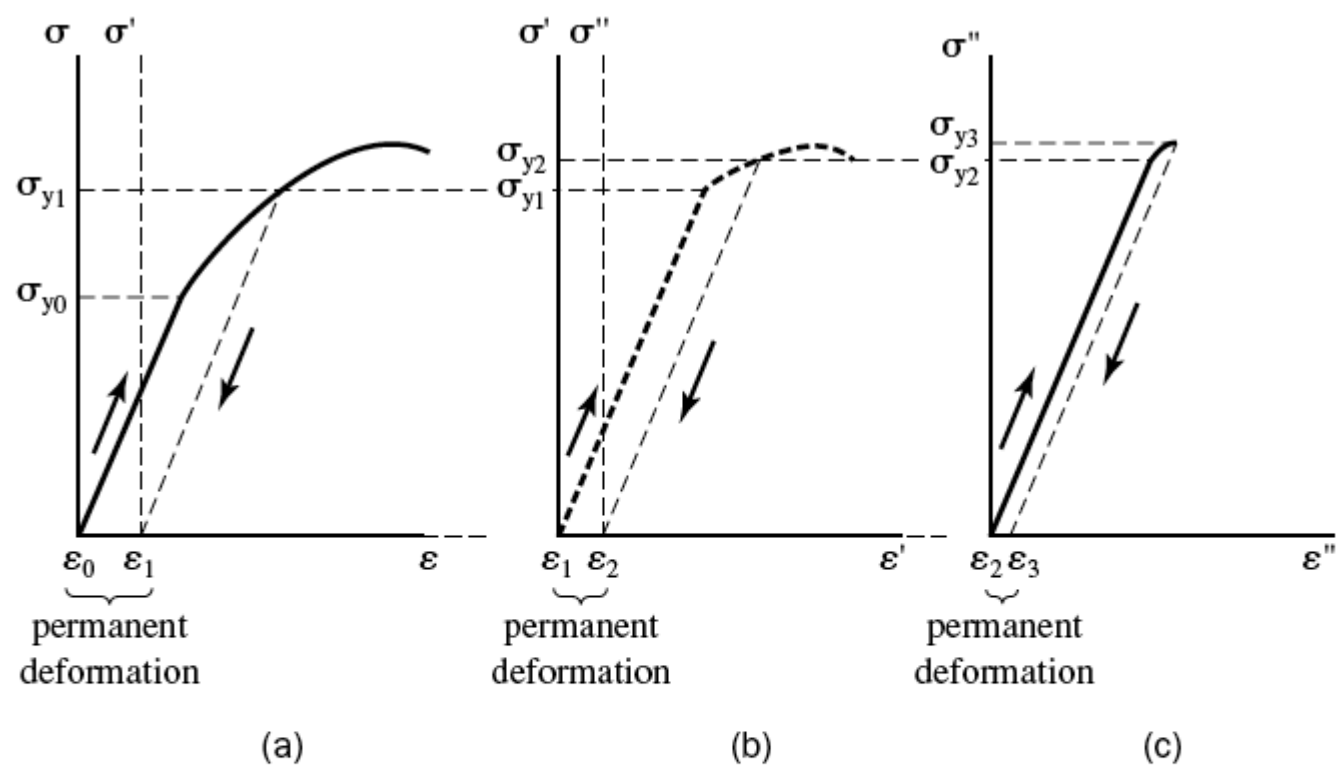
causes a far-reaching elastic distortion of the lattice as well as a severe distortion in the vicinity of the end point of the inserted plane. The locus where the half-plane terminates is defined to be the *dislocation line* [Figure 3.21(a)]. It is depicted by the symbol \perp , where the vertical line represents the extra half-plane and the horizontal line the *slip plane*; see Figure 3.21. (An edge dislocation involving an extra half-plane of atoms in the bottom portion of a crystal is designated by τ .)

The insertion of an extra half-plane is by no means limited to the atomic scale. Indeed, these types of deviations from regular structures can be found quite frequently in nature. Figure 3.22 presents, as an example, a corn cob which shows an extra half-row of kernels squeezed between an otherwise nearly regular pattern.

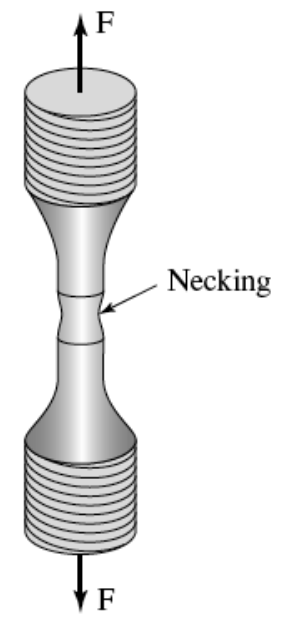
If a shear stress above the critical resolved shear stress is applied to a crystal as indicated in Figure 3.20, the distortion of the lattice in the vicinity of an edge dislocation allows the bonds between the involved atoms to break. This is shown as an exam-

FCC $\{111\} \langle 110 \rangle$

four $\{111\}$ planes and three $[110]$ directions for each plane
 FCC slip system has 12 preferred slip systems



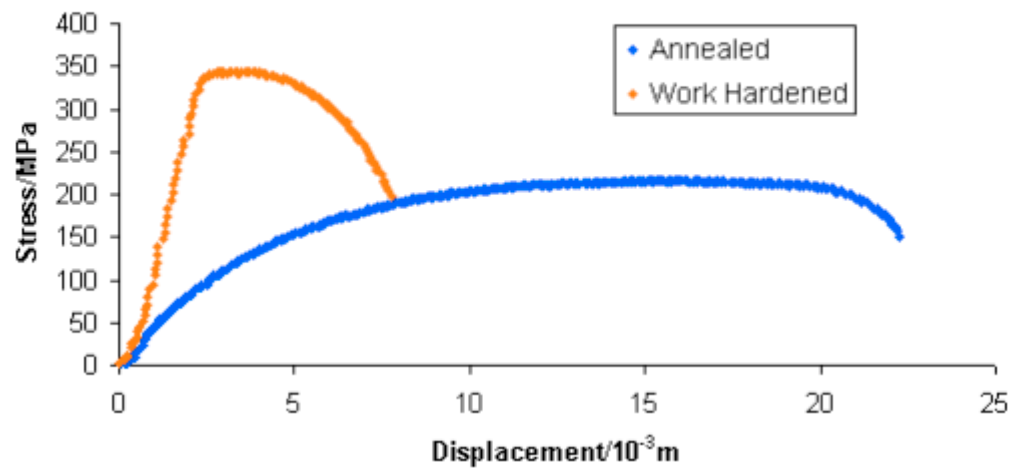
$$\sigma = \frac{F}{A}, \quad \epsilon = \frac{\Delta L}{L}$$



Trapped Dislocations
 lead to Strain Hardening

FIGURE 2.8. Increase of yield strength (and reduction of ductility) by repeated plastic deformation. (a) Sample is moderately stressed until some plastic deformation has occurred, and then it is unloaded, which yields permanent deformation. (b) The sample is subsequently additionally permanently deformed. Note that the coordinate system has shifted after unloading from ϵ_0 to ϵ_1 . (c) Limit of plastic deformation is reached after renewed stressing.

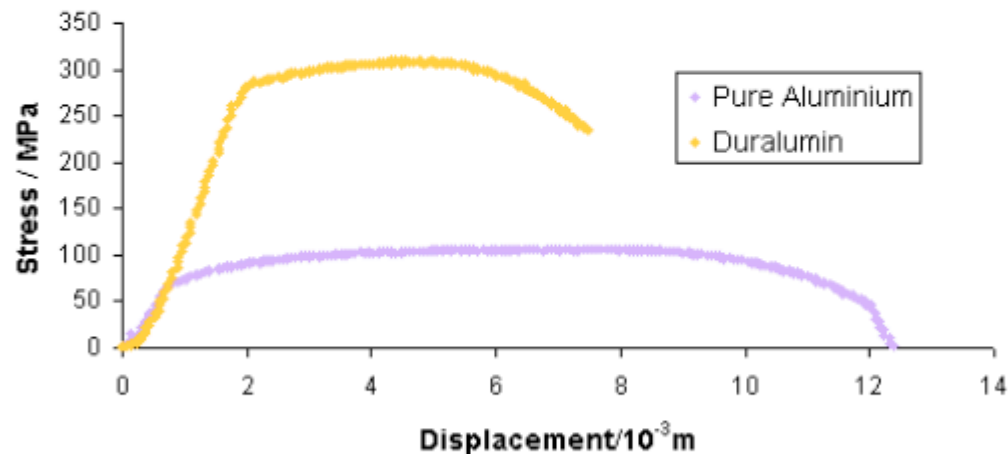
Graph showing stress against displacement for copper samples in tensile tests



Precipitation Hardening

In Duralumin copper forms precipitates of CuAl_2 within an aluminum matrix - see image below. These precipitates hinder the movement of dislocations and substantially strengthen the alloy. This process is widely used to make strong aluminum alloys for structural purposes, and is known as precipitation hardening.

Graph showing stress against displacement for aluminium and duralumin samples in tensile tests



The yield stress for aluminium is about a quarter that for duralumin, because there is far less resistance to the movement of the dislocations in pure aluminium. In the alloy the precipitates hinder the motion of the dislocations and a much higher stress is required to initiate slip.

<http://www.exo.net/~jillj/activities/mechanical.pdf>

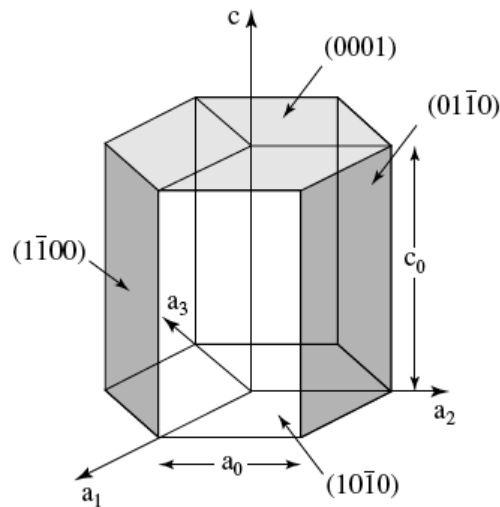
FCC $\{111\} \langle 110 \rangle$

four $\{111\}$ planes and three $\langle 110 \rangle$ directions for each plane
 FCC slip system has 12 preferred slip systems

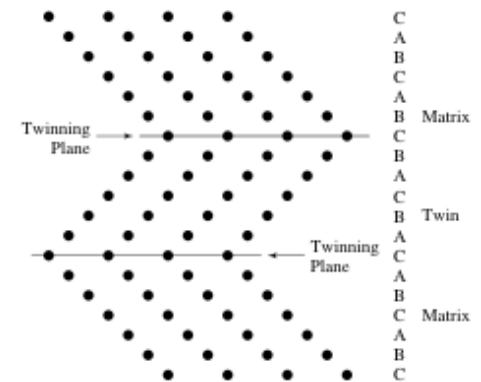
hand, there are enough possible slip systems so that at least one of them can always be activated under essentially any direction of applied stress. On the other hand, the number of slip systems is not excessively large so as to cause initially mutual blocking of adjacent dislocation movements. Since FCC metals have an optimum number of slip systems, they can be easily deformed and are therefore ductile.

HCP $\{0001\} \langle 1000 \rangle$

One $\{0001\}$ planes and three $\langle 1000 \rangle$ directions for each plane
 HCP slip system has 3 preferred slip systems

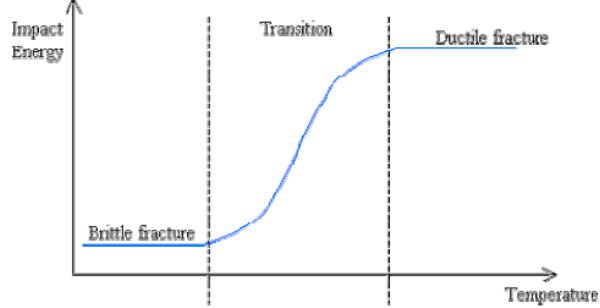


Twinning can easily occur in HCP

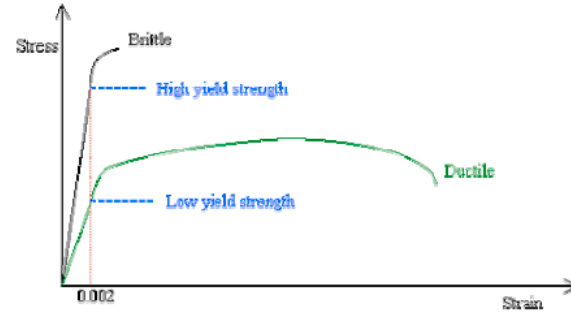


Generally HCP is brittle due to too few slip systems

I. Ductile to Brittle Transition Temperature



The ductile-brittle transition is exhibited in bcc metals, such as low carbon steel, which become brittle at low temperature or at very high strain rates. FCC metals, however, generally remain ductile at low temperatures.



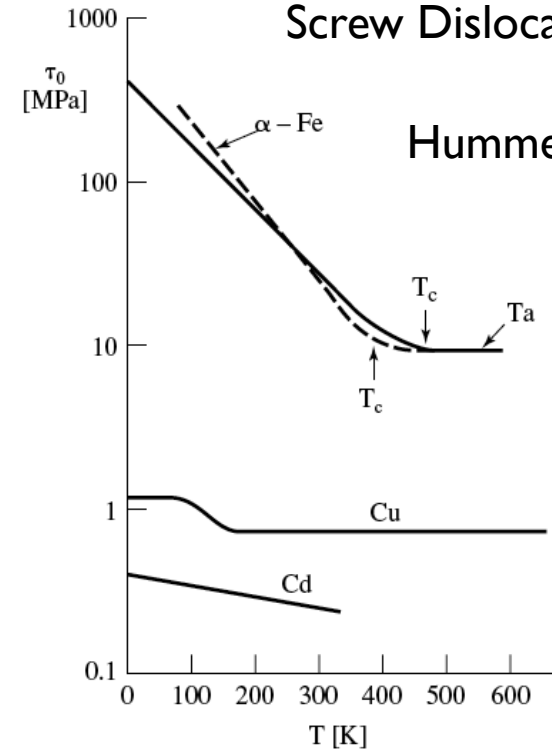
The area under the stress-strain curve gives the fracture energy of the material. A ductile material has a greater fracture energy.

BCC

BCC has no closest-packed planes
 Slip occurs on “nearly” closest packed planes
 48 near slip systems
 (slip direction is closest packed $\langle 111 \rangle$)
 Extensive “locking-in” of slip systems
 Somewhat ductile and strong
 Screw Dislocations are more important
 than edge dislocations

FIGURE 3.23. Schematic representation of the temperature-dependence of the critical resolved shear stress, τ_0 , for Ta (BCC), α -Fe (BCC), Cu (FCC), and Cd (HCP) single crystals. Since τ_0 depends strongly on the crystal orientation, an *average orientation* has been chosen. Specifically, the tensile direction has about the same angle to the [100], [110], and [111] crystal axes. Note the logarithmic scale on the y axis.

Thermally Activated Screw Dislocations



Hummel P. 53

Hummel 54

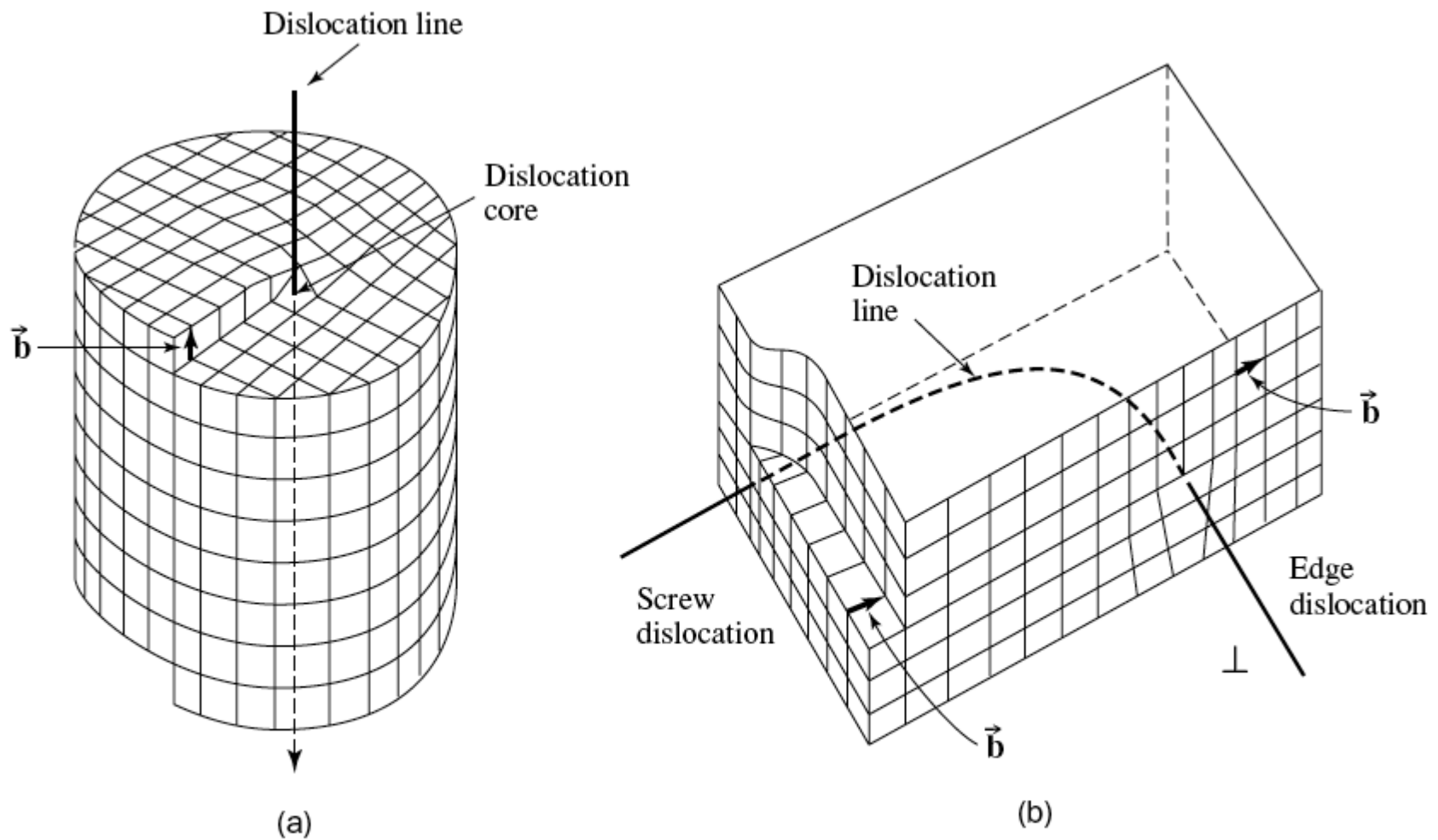


FIGURE 3.24. Schematic representations of (a) a screw dislocation and (b) mixed dislocations for which the edge and the screw dislocations are extreme cases.

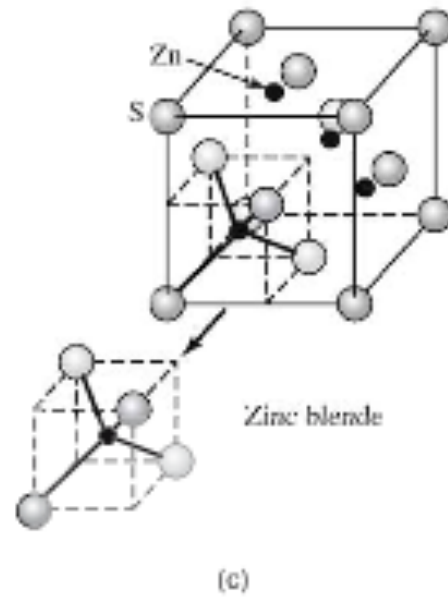
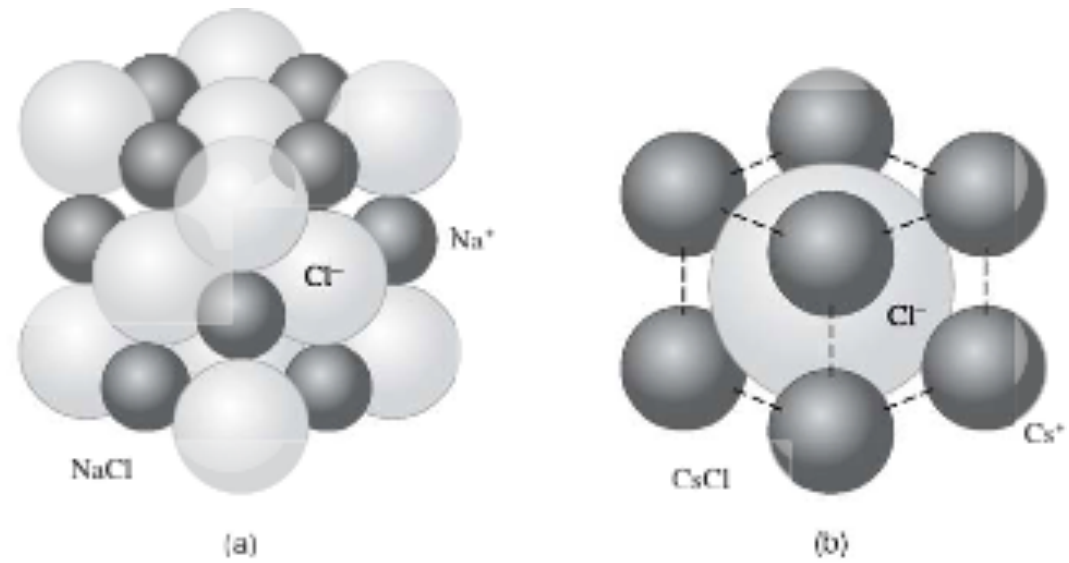


FIGURE 3.18. Some characteristic ceramic crystal structures.

Polymer Crystals

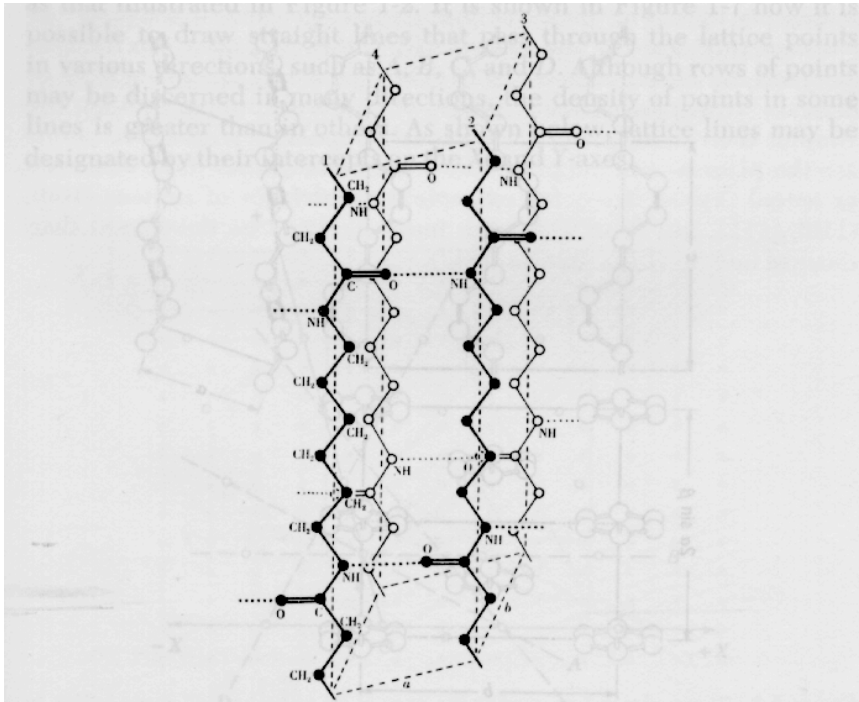


Figure 1-5 Arrangement of molecular chains in nylon 66, poly(hexamethylene adipamide). (Bunn and Garner [6].)

Nylon 66, from Alexander, "X-Ray Diffraction Methods in Polymer Science"

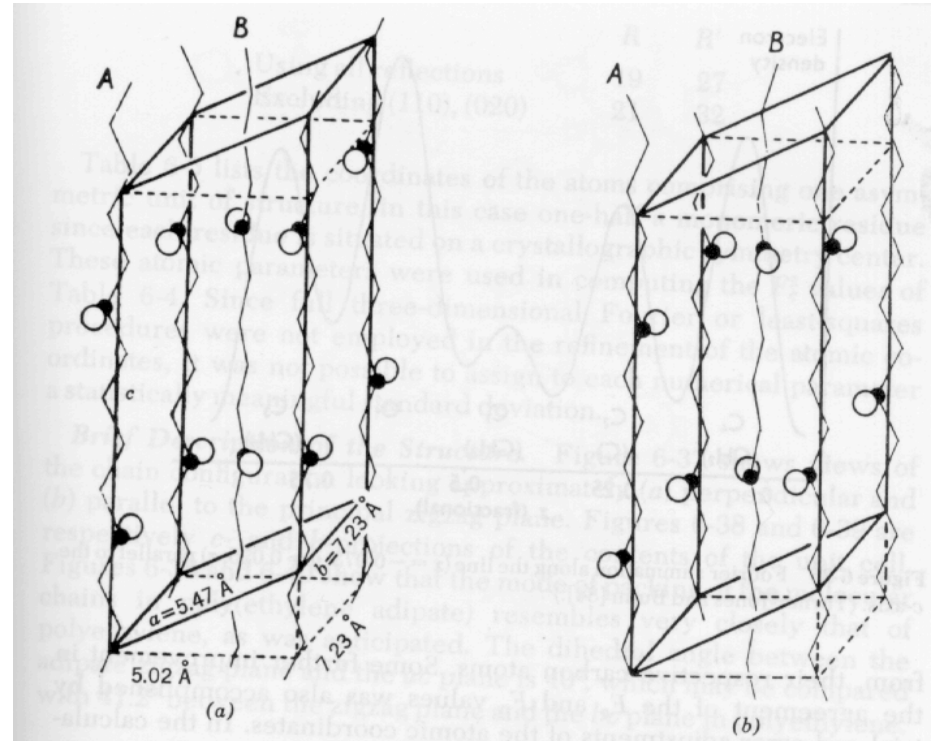
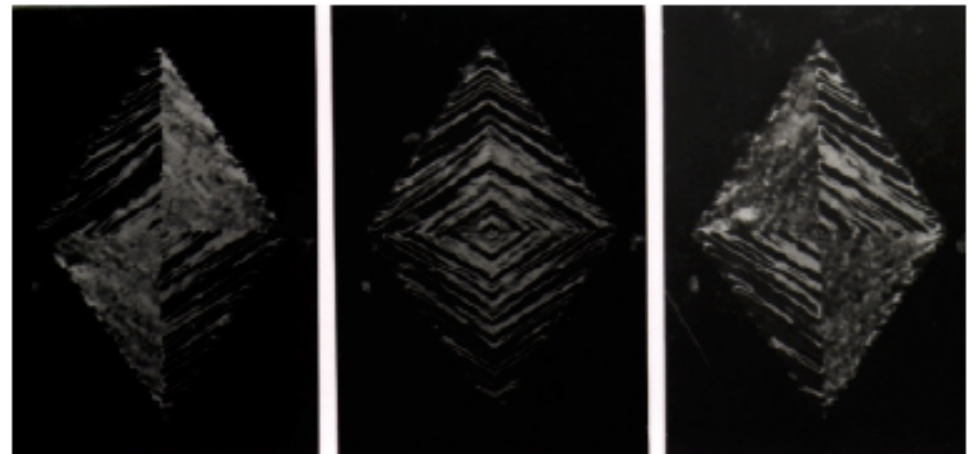
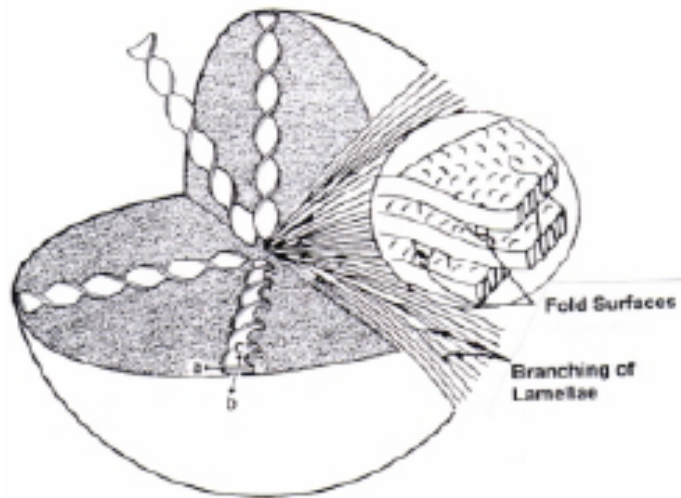
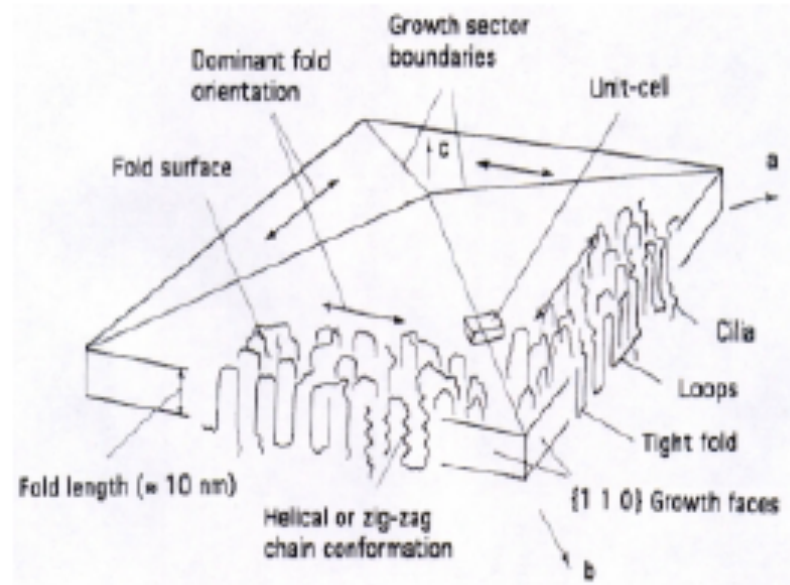
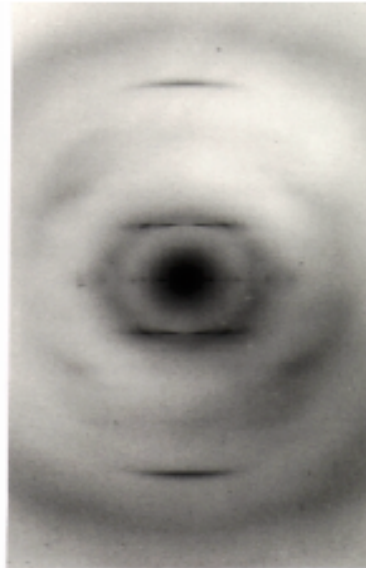
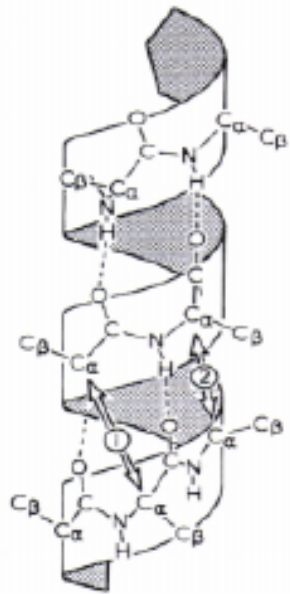
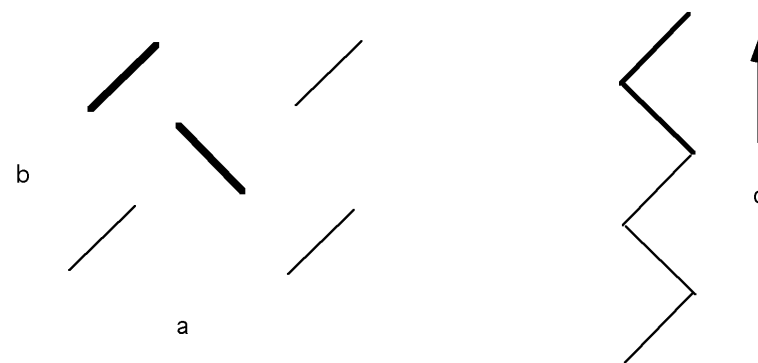
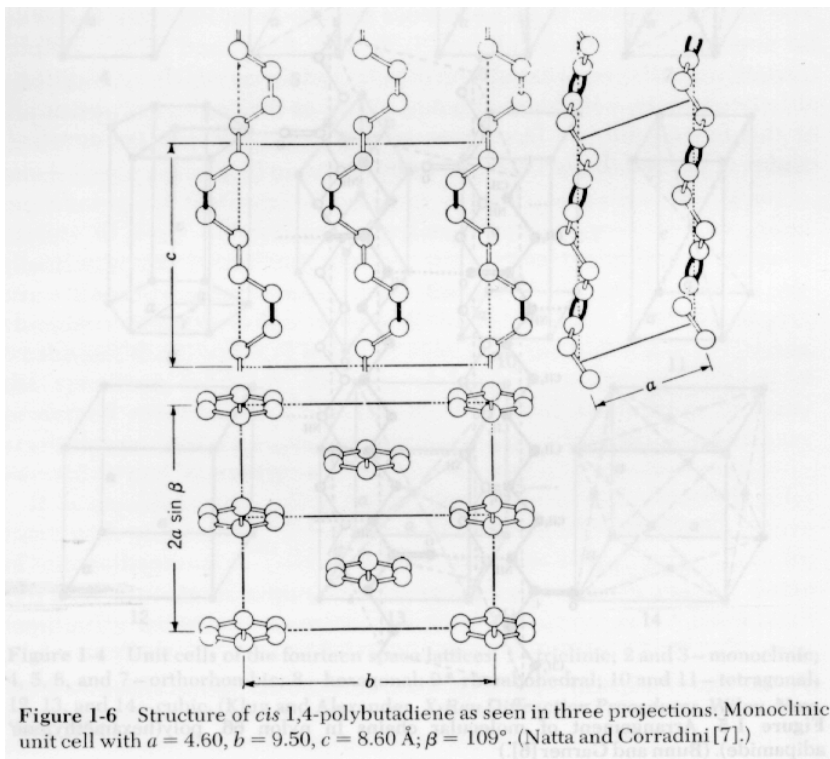


Figure 6-35 Unit cell of poly(ethylene adipate) and the two possible orientations of the molecular chain. (Turner-Jones and Bunn [84].)

Poly(ethylene adipate), a polyester, from Alexander, "X-Ray Diffraction Methods in Polymer Science"

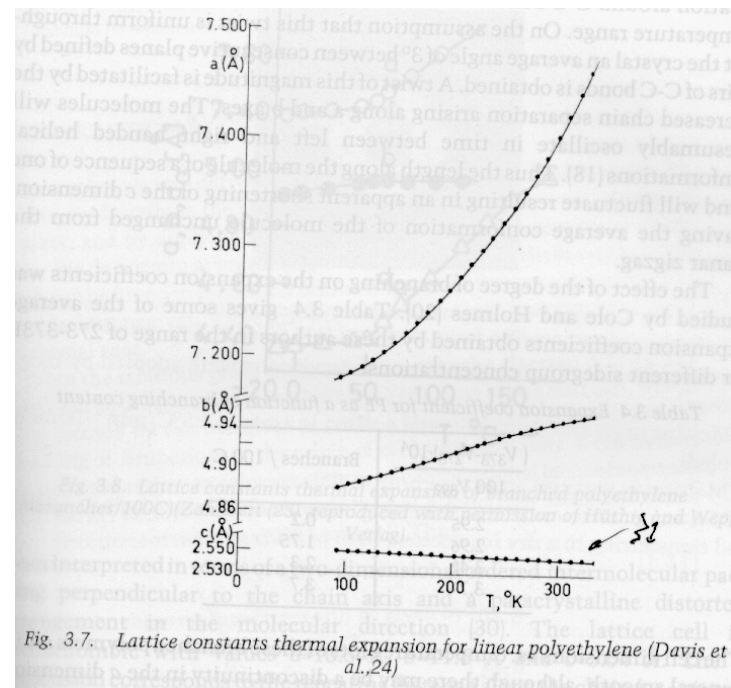
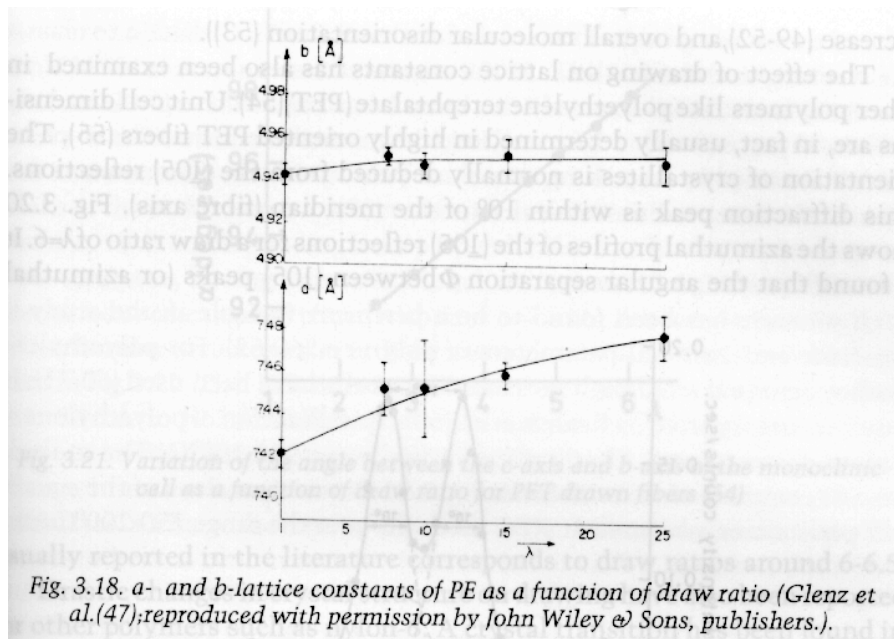
From B. Lotz paper





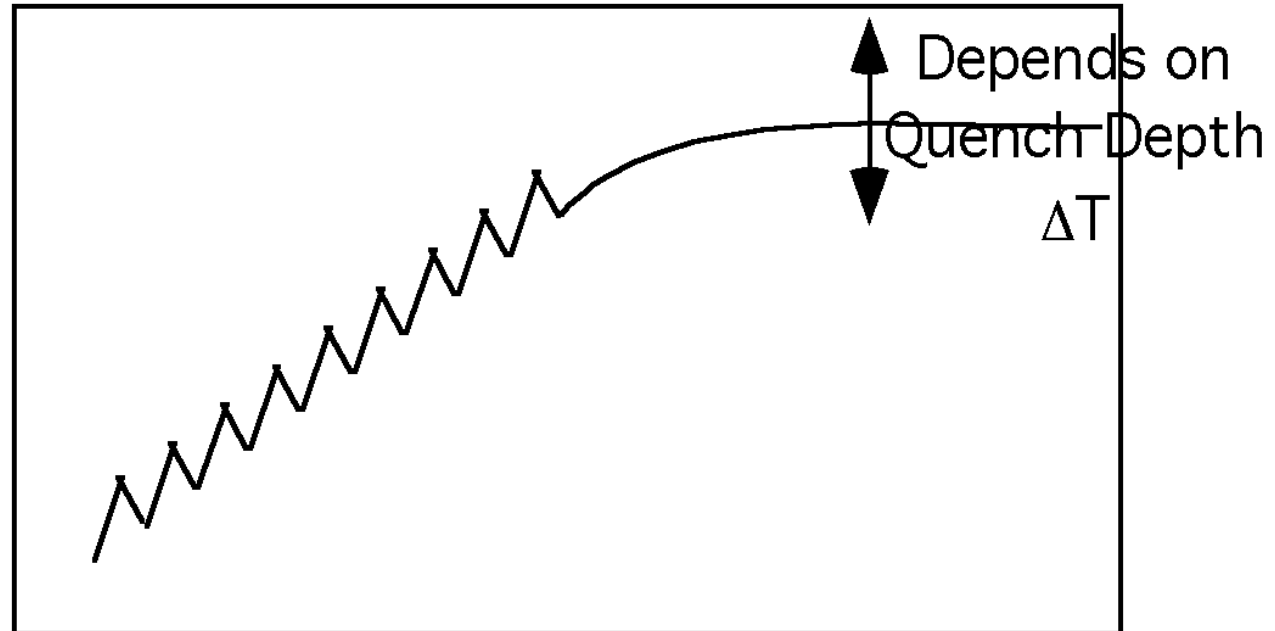
Polyethylene and alkane waxes

Polybutadiene (PBD), from Alexander, "X-Ray Diffraction Methods in Polymer Science"



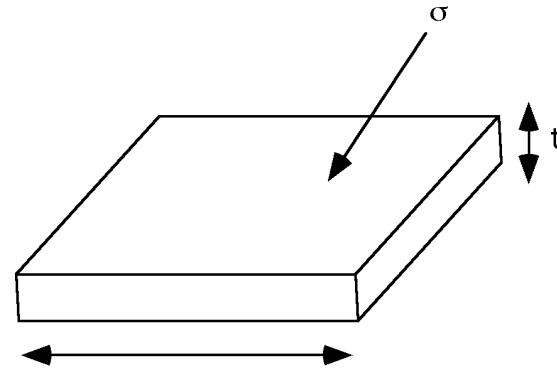
Alkanes and Polyethylene

Crystallite Thickness



Number of mer units

$$t = \frac{2\sigma_e T_{m,\infty}}{\Delta H_f (T_{m,\infty} - T_{m,t})}$$



Hoffman-Lauritzen Equation^R (a form of the Gibbs-Thompson Equation)

Consider a crystal where $t \Rightarrow \infty$

$$\Delta G_{f,T_\infty} = 0 = \Delta H_f - T_\infty \Delta S_f$$

$$\Delta S_f = \frac{\Delta H_f}{T_\infty}$$

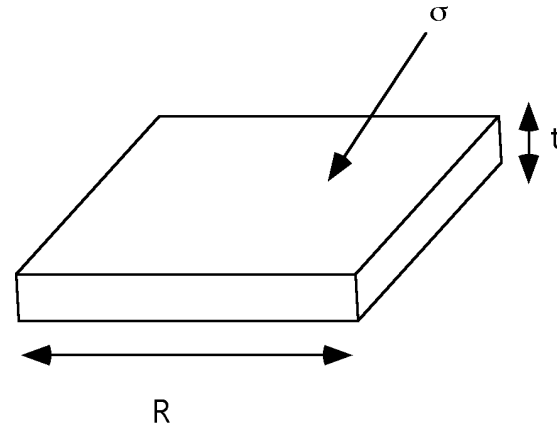
Consider a crystal where t is finite crystallized at $T_{m,t}$ (Gibbs Pseudo-Equilibrium Assumption)

$$V \Delta G_{f,T_{m,t}} = 0 = V (\Delta H_f - T_{m,\infty} \Delta S_f) - 2R^2 \sigma_e$$

$$t R^2 \Delta H_f \left(\frac{T_{m,\infty} - T_{m,t}}{T_{m,\infty}} \right) = 2R^2 \sigma_e$$

$$t = \frac{2\sigma_e T_{m,\infty}}{\Delta H_f (T_{m,\infty} - T_{m,t})}$$

$$t = \frac{2\sigma_e T_{m,\infty}}{\Delta H_f (T_{m,\infty} - T_{m,t})}$$



Hoffman-Lauritzen Equation (a form of the Gibbs-Thompson Equation)

The further crystallization occurs from equilibrium (deeper the quench)
The smaller the nano-crystal

This is the basic rule of nanomaterials (could be called “*Gibb’s Law*”)
Nanoparticles are formed far from equilibrium.

Good sources of nanoparticles are bursts of concentration, explosions, jet engine exhaust, diesel/
gasoline engine exhaust, high temperature flames,
conditions where you find rapid supersaturation of a condensing species.



Bassett Polymer Crystals

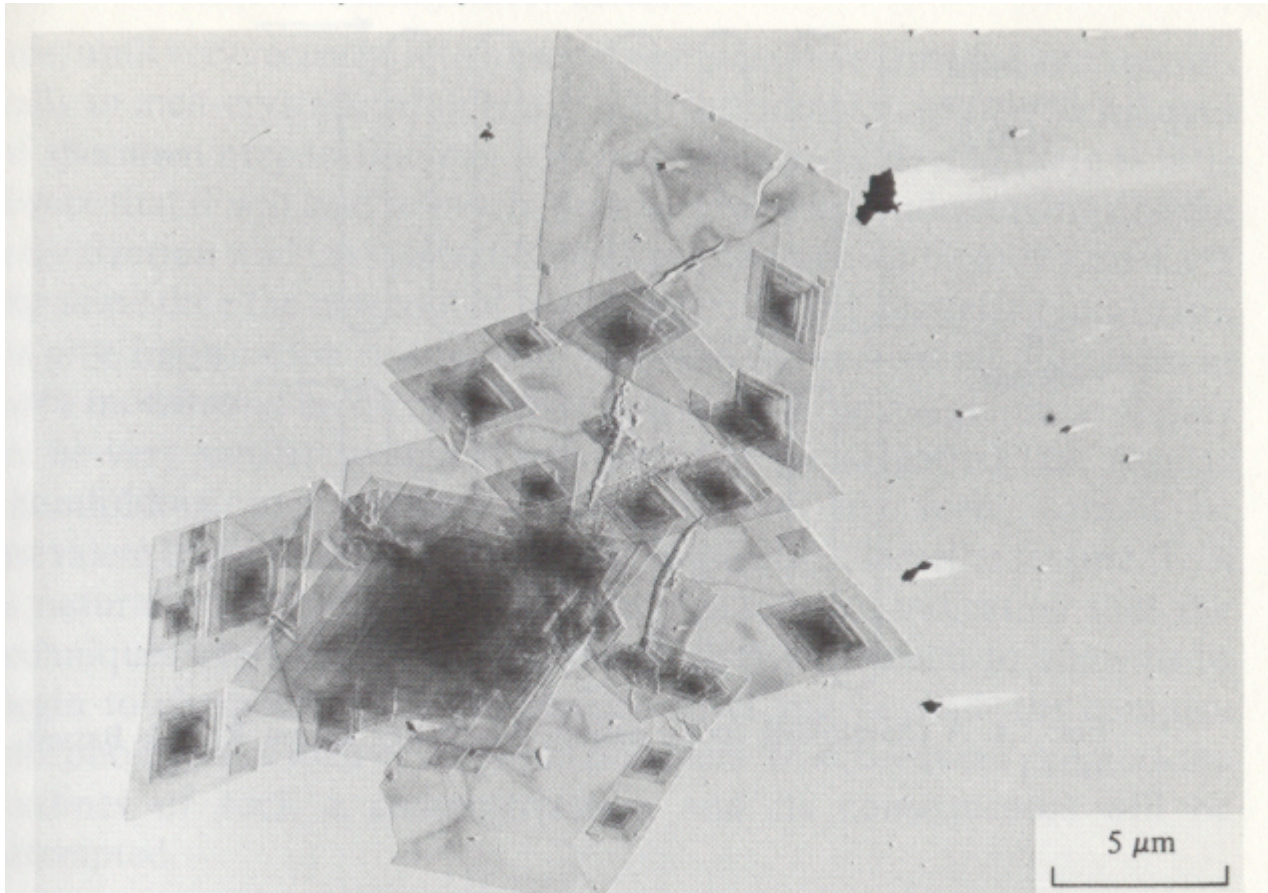


Fig. 1.3. Solution-grown lamellae of polyethylene. Among their many features are an internal step and change of habit due to a fall in crystallization temperature, evidence of sectors and non-planarity and the development of growth spirals as planar growth surfaces become unstable.

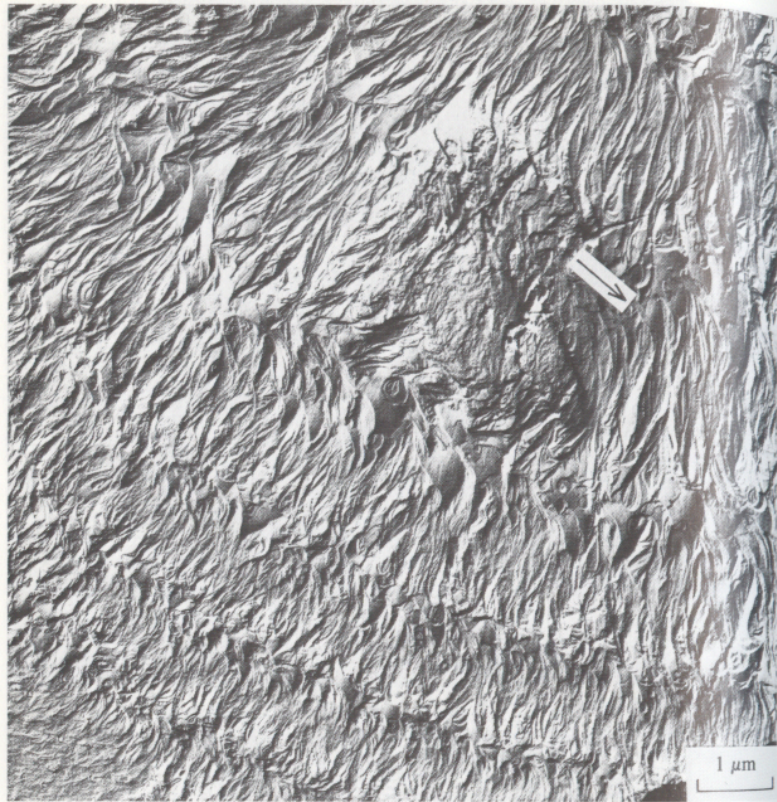


Fig. 4.34. An apparently diametral section of a similar banded polyethylene spherulite to that of Fig. 4.33. Note the splitting of lamellae (arrowed centre right). Etched surface. (From Bassett & Hodge, 1978*a*.)



Fig. 4.36. Microstructure of a commercial polyethylene (Rigidex 50) crystallized at 119.8 °C which contains S-shaped, planar and ridged lamellae. Etched surface. (From Bassett, Hodge & Olley, 1979.)

26 *Spherulites*

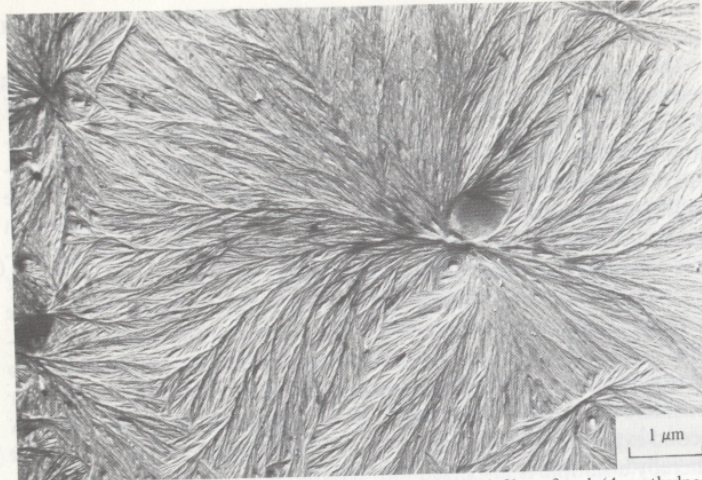
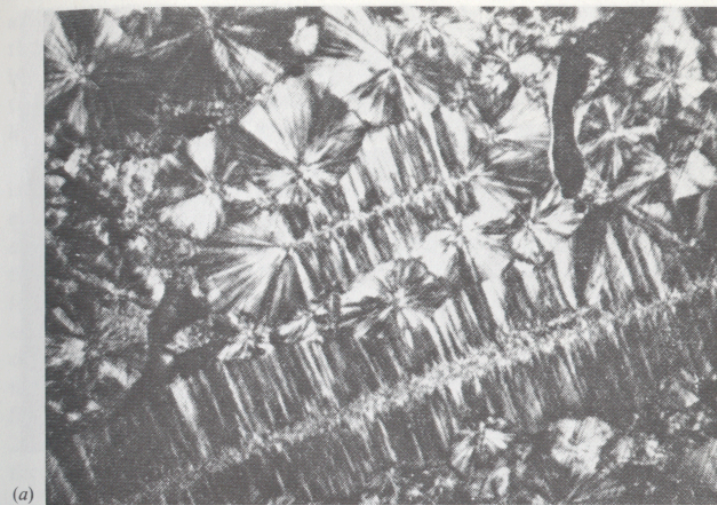


Fig. 2.6. Spherulitic sheaf in a melt-crystallized film of poly(4-methylpentene-1).

2.1 *Spherulitic morphologies*

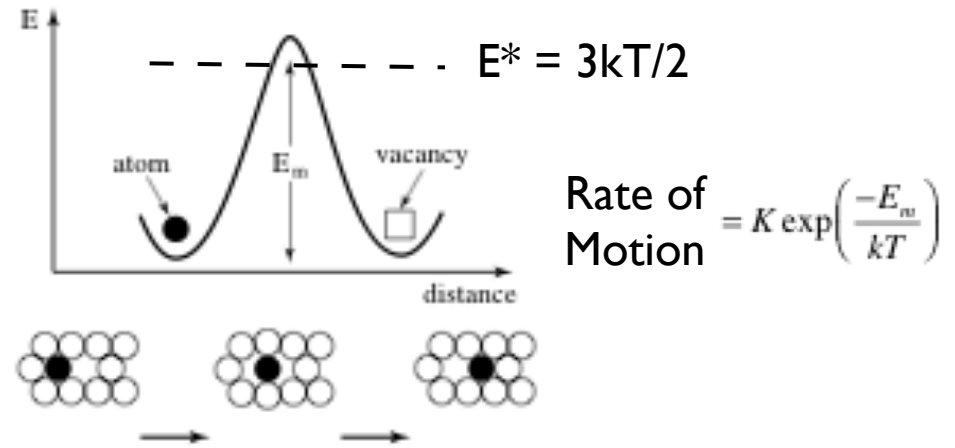


Crystallization

Locally we see that atoms must overcome energy barriers to move both in the crystalline (solid) and in the amorphous (liquid) state.

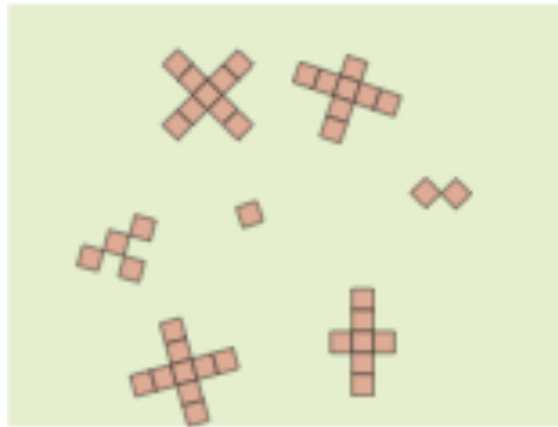
from Hummel Text p. 104

FIGURE 6.1. Schematic representation of the diffusion of an atom from its former position into a vacant lattice site. An activation energy for motion, E_m , has to be applied which causes a momentary and local expansion of the lattice to make room for the passage of the atom. This two-dimensional representation shows only part of the situation. Atoms above and below the depicted plane may contribute likewise to diffusion.

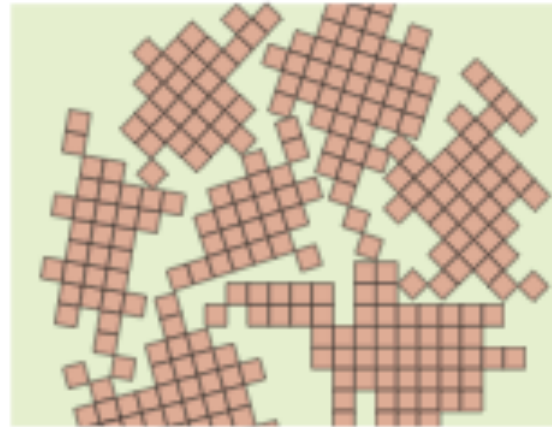


As temperature drops E^* drops until atoms can not easily move beyond their crystalline positions due to a coordinated organization of all of the atoms at the crystallization point. Similarly, on heating E^* rises and overcomes the energy barrier allowing for motion of atoms at the melting point. Since crystallization and melting require coordinated motion of all of the atoms in a self enhancing manner (the more atoms move the easier it is for other atoms to move) we observe a discrete, first order transition (an abrupt change in order, volume, density, heat content).

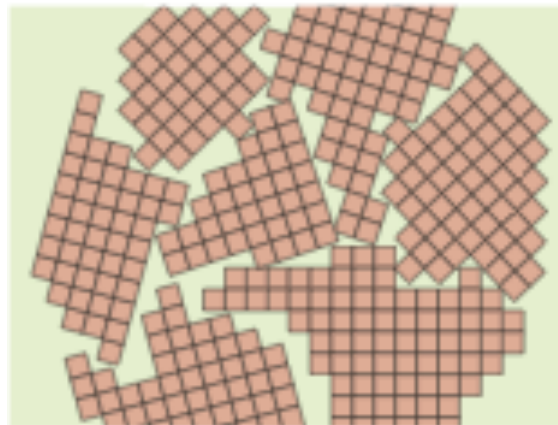
Grains



(a)



(b)



(c)



(d)

Figure 3.17 Schematic diagrams of the various stages in the solidification of a polycrystalline material; the square grids depict unit cells. (a) Small crystallite nuclei. (b) Growth of the crystallites; the obstruction of some grains that are adjacent to one another is also shown. (c) Upon completion of solidification, grains having irregular shapes have formed. (d) The grain structure as it would appear under the microscope; dark lines are the grain boundaries. (Adapted from W. Rosenhain, *An Introduction to the Study of Physical Metallurgy*, 2nd edition, Constable & Company Ltd., London, 1915.)

Galvanized steel (hot dip zinc coating or electrochemically)



Control Grain size with number of seeds for nucleation
manipulation of growth rate vs nucleation rate with temperature/additives

Generally grains are too small to see $\sim 1 \mu\text{m}$

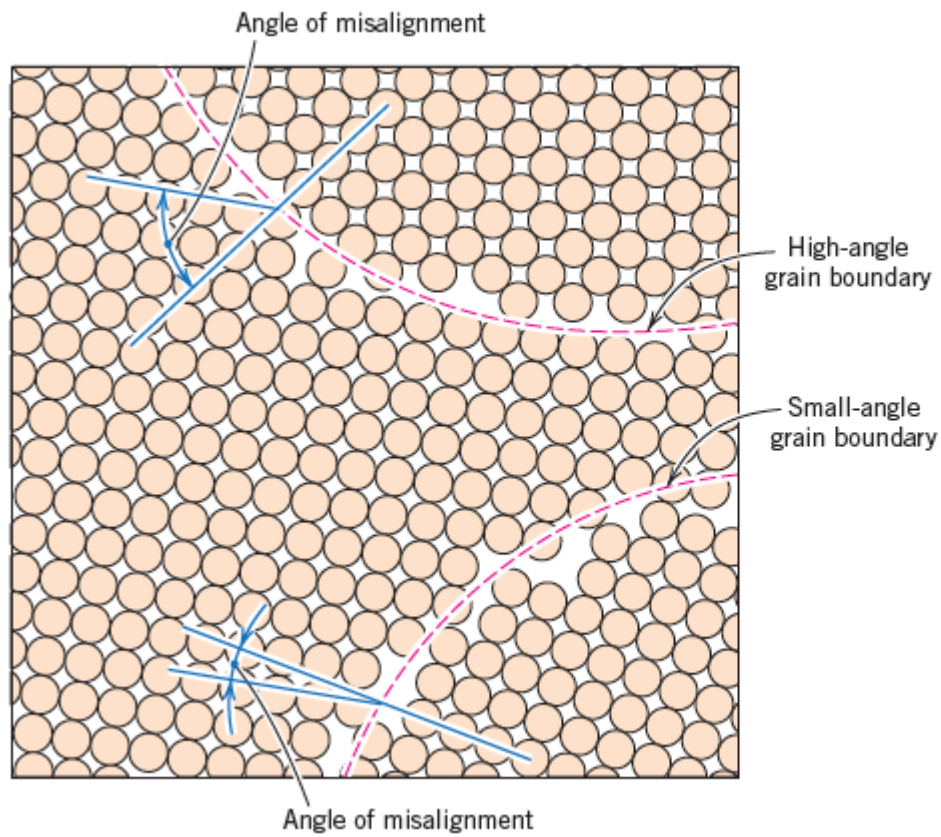


Figure 4.7 Schematic diagram showing small- and high-angle grain boundaries and the adjacent atom positions.

Different mechanical behavior is expected from high and low angle grain boundaries

Drawn Aluminum Sheet



Hall-Petch Relationship for Multigrain Metals

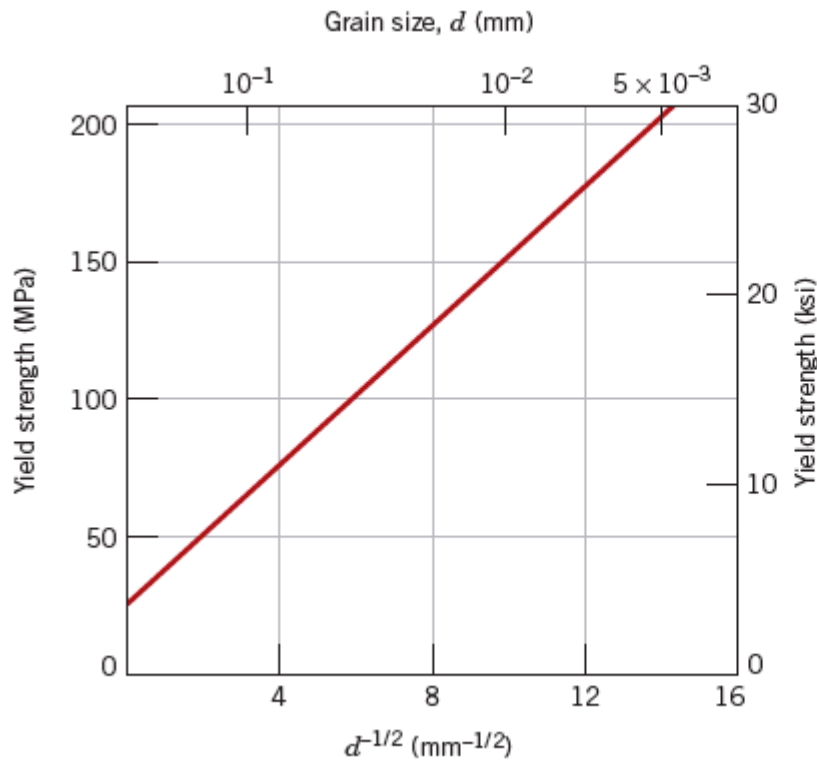


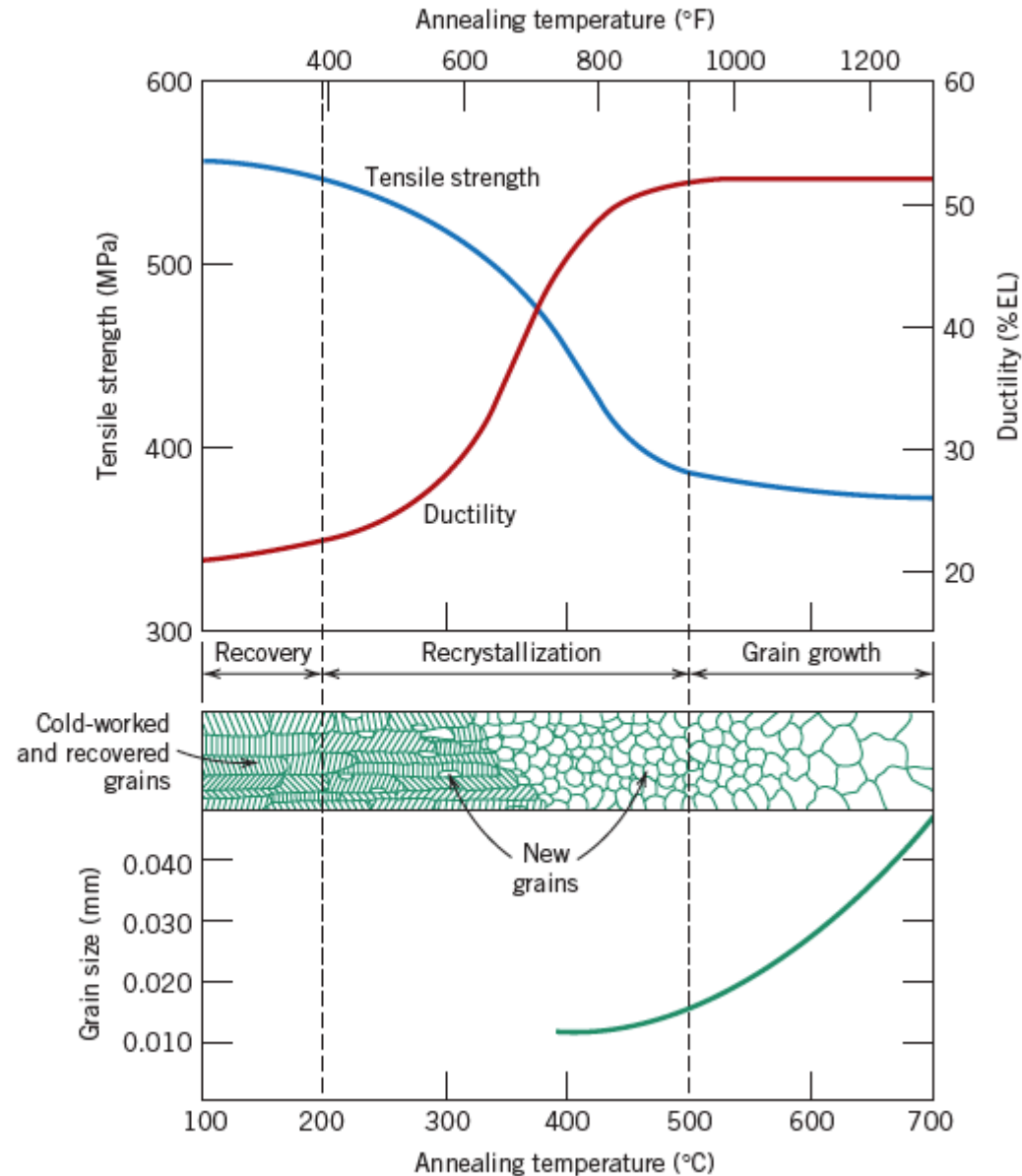
Figure 7.15 The influence of grain size on the yield strength of a 70 Cu–30 Zn brass alloy. Note that the grain diameter increases from right to left and is not linear. (Adapted from H. Suzuki, “The Relation Between the Structure and Mechanical Properties of Metals,” Vol. II, *National Physical Laboratory, Symposium No. 15*, 1963, p. 524.)

Callister P. 189

$$\sigma_y = \sigma_0 + \frac{k}{\sqrt{d}}$$

Hummel P. 58

Figure 7.22 The influence of annealing temperature (for an annealing time of 1 h) on the tensile strength and ductility of a brass alloy. Grain size as a function of annealing temperature is indicated. Grain structures during recovery, recrystallization, and grain growth stages are shown schematically. (Adapted from G. Sachs and K. R. Van Horn, *Practical Metallurgy, Applied Metallurgy and the Industrial Processing of Ferrous and Nonferrous Metals and Alloys*, American Society for Metals, 1940, p. 139.)



Callister, P. 213

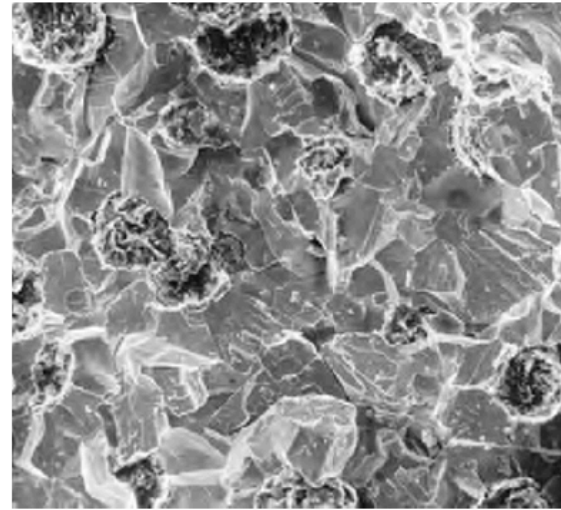
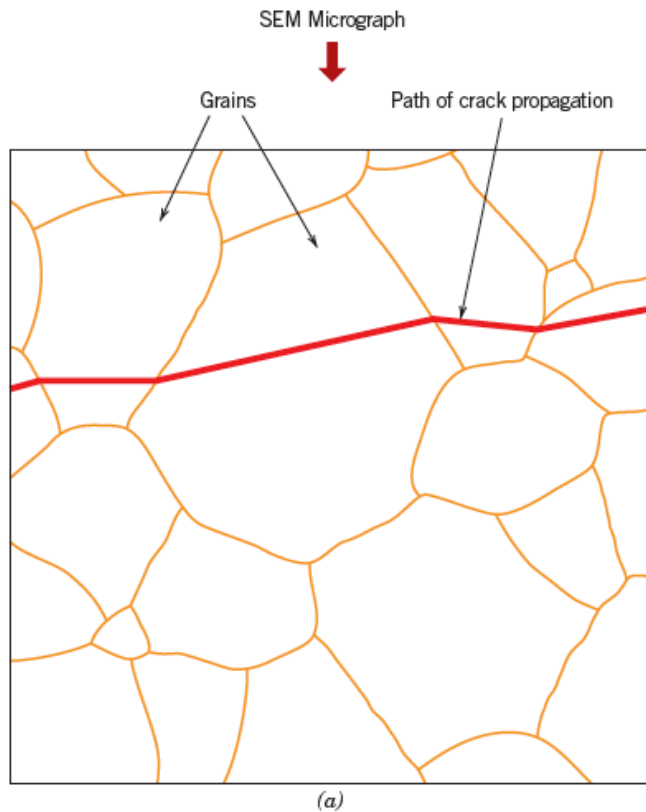


Figure 8.6 (a) Schematic cross-section profile showing crack propagation through the interior of grains for transgranular fracture. (b) Scanning electron fractograph of ductile cast iron showing a transgranular fracture surface. Magnification unknown. [Figure (b) from V. J. Colangelo and F. A. Heiser, *Analysis of Metallurgical Failures*, 2nd edition. Copyright © 1987 by John Wiley & Sons, New York. Reprinted by permission of John Wiley & Sons, Inc.]